Fractional topological insulators

Christopher Mudry[1] Titus Neupert[1] Claudio Chamon[2] Luiz Santos[3] Shinsei Ryu[4]

[1]Paul Scherrer Institut, Switzerland

[2]Boston University, USA

[3]Harvard University, USA

[4]University of Illinois, Urbana-Champaign, USA

Frascati, 07 September 2011

Outline

Strong interacting limit in the jellium model

The (quantum) jellium model in a box of volume V is defined by

$$\widehat{H} = \sum_{i=1}^{N_{\mathrm{e}}} \frac{\widehat{\boldsymbol{p}}_i^2}{2m_{\mathrm{e}}} + \frac{1}{V}\sum_{\boldsymbol{q}\neq\boldsymbol{0}} \frac{2\pi e^2}{\boldsymbol{q}^2}\left(\widehat{\rho}_{+\boldsymbol{q}}\widehat{\rho}_{-\boldsymbol{q}} - N_{\mathrm{e}}\right), \qquad \widehat{\rho}_{+\boldsymbol{q}} := \sum_{i=1}^{N_{\mathrm{e}}} e^{-\mathrm{i}\boldsymbol{q}\cdot\widehat{\boldsymbol{r}}_i}.$$

The parameter

$$r_{\mathrm{s}} := \frac{e^2/a}{\hbar^2/(2m_{\mathrm{e}}a^2)} \equiv \frac{a}{a_{\mathrm{B}}} \quad \text{where} \quad a := \left(\frac{N_{\mathrm{e}}}{V}\right)^{-1/3}$$

measures the relative strength between the Coulomb and the kinetic energy.

The ground state is a featureless compressible liquid when $r_{\mathrm{s}} \ll 1$, i.e., the Fermi liquid.

The ground state breaks spontaneously translation invariance when $r_{\mathrm{s}} \gg 1$ by forming a Wigner crystal.

Strong interacting limit in the jellium model

The (quantum) jellium model in a box of volume V is defined by

$$\widehat{H} = \sum_{i=1}^{N_{\mathrm{e}}} \frac{\widehat{\boldsymbol{p}}_i^2}{2m_{\mathrm{e}}} + \frac{1}{V} \sum_{\boldsymbol{q}\neq\boldsymbol{0}} \frac{2\pi e^2}{\boldsymbol{q}^2} \left(\widehat{\rho}_{+\boldsymbol{q}}\widehat{\rho}_{-\boldsymbol{q}} - N_{\mathrm{e}}\right), \qquad \widehat{\rho}_{+\boldsymbol{q}} := \sum_{i=1}^{N_{\mathrm{e}}} e^{-\mathrm{i}\boldsymbol{q}\cdot\widehat{\boldsymbol{r}}_i}.$$

The parameter

$$r_{\mathrm{s}} := \frac{e^2/a}{\hbar^2/(2m_{\mathrm{e}}a^2)} \equiv \frac{a}{a_{\mathrm{B}}} \quad \text{where} \quad a := \left(\frac{N_{\mathrm{e}}}{V}\right)^{-1/3}$$

measures the relative strength between the Coulomb and the kinetic energy.

The ground state is a featureless compressible liquid when $r_{\mathrm{s}} \ll 1$, i.e., the Fermi liquid.

The ground state breaks spontaneously translation invariance when $r_{\mathrm{s}} \gg 1$ by forming a Wigner crystal.

Strong interacting limit in the jellium model

The (quantum) jellium model in a box of volume V is defined by

$$\widehat{H}=\sum_{i=1}^{N_{\mathrm{e}}}\frac{\widehat{\boldsymbol{p}}_i^2}{2m_{\mathrm{e}}}+\frac{1}{V}\sum_{\boldsymbol{q}\neq\boldsymbol{0}}\frac{2\pi e^2}{\boldsymbol{q}^2}\left(\widehat{\rho}_{+\boldsymbol{q}}\widehat{\rho}_{-\boldsymbol{q}}-N_{\mathrm{e}}\right), \qquad \widehat{\rho}_{+\boldsymbol{q}}:=\sum_{i=1}^{N_{\mathrm{e}}}e^{-\mathrm{i}\boldsymbol{q}\cdot\widehat{\boldsymbol{r}}_i}.$$

The parameter

$$r_{\mathrm{s}}:=\frac{e^2/a}{\hbar^2/(2m_{\mathrm{e}}a^2)}\equiv\frac{a}{a_{\mathrm{B}}} \quad \text{where} \quad a:=\left(\frac{N_{\mathrm{e}}}{V}\right)^{-1/3}$$

measures the relative strength between the Coulomb and the kinetic energy.

The ground state is a featureless compressible liquid when $r_{\mathrm{s}}\ll 1$, i.e., the Fermi liquid.

The ground state breaks spontaneously translation invariance when $r_{\mathrm{s}}\gg 1$ by forming a Wigner crystal.

Strong interacting limit in the jellium model

The (quantum) jellium model in a box of volume V is defined by

$$\widehat{H}=\sum_{i=1}^{N_{\mathrm{e}}}\frac{\widehat{\boldsymbol{p}}_i^2}{2m_{\mathrm{e}}}+\frac{1}{V}\sum_{\boldsymbol{q}\neq\boldsymbol{0}}\frac{2\pi e^2}{\boldsymbol{q}^2}\left(\widehat{\rho}_{+\boldsymbol{q}}\widehat{\rho}_{-\boldsymbol{q}}-N_{\mathrm{e}}\right),\qquad \widehat{\rho}_{+\boldsymbol{q}}:=\sum_{i=1}^{N_{\mathrm{e}}}e^{-\mathrm{i}\boldsymbol{q}\cdot\widehat{\boldsymbol{r}}_i}.$$

The parameter

$$r_{\mathrm{s}}:=\frac{e^2/a}{\hbar^2/(2m_{\mathrm{e}}a^2)}\equiv\frac{a}{a_{\mathrm{B}}}\quad\text{where}\quad a:=\left(\frac{N_{\mathrm{e}}}{V}\right)^{-1/3}$$

measures the relative strength between the Coulomb and the kinetic energy.

The ground state is a featureless compressible liquid when $r_{\mathrm{s}}\ll 1$, i.e., the Fermi liquid.

The ground state breaks spontaneously translation invariance when $r_{\mathrm{s}}\gg 1$ by forming a Wigner crystal.

2-dimensional Jellium model in a strong magnetic field

Assume the presence of a uniform magnetic field $B\,\hat{\boldsymbol{z}}$ and of a confining potential along the $\hat{\boldsymbol{z}}$ direction, so that the single-particle electronic levels are Landau levels.

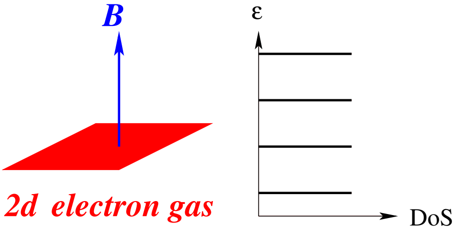

The filling fraction of the Landau levels is the number

$$\nu := \frac{n\,h\,c}{e\,B}$$

where n is the 2-dimensional electron density.

2-dimensional Jellium model in a strong magnetic field

Assume the presence of a uniform magnetic field $B\,\widehat{\boldsymbol{z}}$ and of a confining potential along the $\widehat{\boldsymbol{z}}$ direction, so that the single-particle electronic levels are Landau levels.

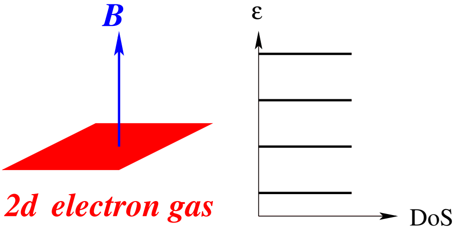

The filling fraction of the Landau levels is the number

$$\nu := \frac{n\,h\,c}{e\,B}$$

where n is the 2-dimensional electron density.

The integer quantum Hall effect

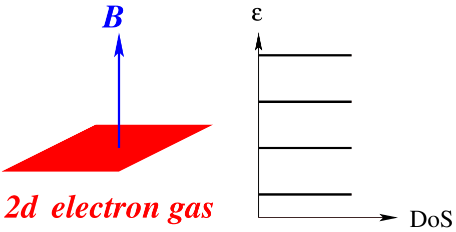

At integer fillings of the Landau levels, the noninteracting ground state is unique and the screened Coulomb interaction V_{int} can be treated perturbatively, as long as transitions between Landau levels or outside the confining potential V_{conf} along the magnetic field are suppressed by the single-particle gaps:

$$V_{\text{int}} \ll \hbar\omega_{\text{c}} \ll V_{\text{conf}}, \qquad \omega_{\text{c}} = eB/(mc).$$

The integer quantum Hall effect

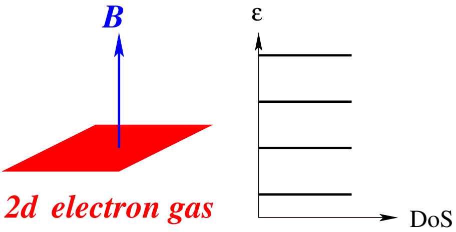

At integer fillings of the Landau levels, the noninteracting ground state is unique and the screened Coulomb interaction $V_{\rm int}$ can be treated perturbatively, as long as transitions between Landau levels or outside the confining potential $V_{\rm conf}$ along the magnetic field are suppressed by the single-particle gaps:

$$V_{\rm int} \ll \hbar\omega_{\rm c} \ll V_{\rm conf}, \qquad \omega_{\rm c} = eB/(mc).$$

The integer quantum Hall effect

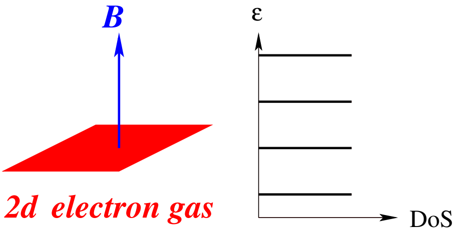

At integer fillings of the Landau levels, the noninteracting ground state is unique and the screened Coulomb interaction $V_{\rm int}$ can be treated perturbatively, as long as transitions between Landau levels or outside the confining potential $V_{\rm conf}$ along the magnetic field are suppressed by the single-particle gaps:

$$V_{\rm int} \ll \hbar\omega_{\rm c} \ll V_{\rm conf}, \qquad \omega_{\rm c} = eB/(mc).$$

The integer quantum Hall effect

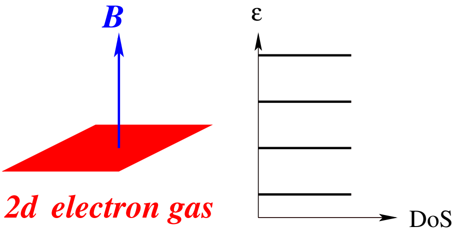

At integer fillings of the Landau levels, the noninteracting ground state is unique and the screened Coulomb interaction V_{int} can be treated perturbatively, as long as transitions between Landau levels or outside the confining potential V_{conf} along the magnetic field are suppressed by the single-particle gaps:

$$V_{\mathrm{int}} \ll \hbar\omega_{\mathrm{c}} \ll V_{\mathrm{conf}}, \qquad \omega_{\mathrm{c}} = eB/(mc).$$

The fractional quantum Hall effect

At fractional fillings of a Landau level, r_s is effectively ∞: A landau level is a massively degenerate flat band of single-particle states.

Naively, one would expect a Wigner crystal (or more exotic ground states with broken symmetry) to be selected by the interaction out of all possible degenerate Slater determinants.

Instead, for "magic" filling fractions, featureless (i.e., liquid like) ground states are selected by the screened Coulomb interaction.

For example, whenever $1/\nu$ is an odd integer, the featureless ground state is an incompressible ground state called a Laughlin state.

The fractional quantum Hall effect

At fractional fillings of a Landau level, r_s is effectively ∞: A landau level is a massively degenerate flat band of single-particle states.

Naively, one would expect a Wigner crystal (or more exotic ground states with broken symmetry) to be selected by the interaction out of all possible degenerate Slater determinants.

Instead, for "magic" filling fractions, featureless (i.e., liquid like) ground states are selected by the screened Coulomb interaction.

For example, whenever $1/\nu$ is an odd integer, the featureless ground state is an incompressible ground state called a Laughlin state.

The fractional quantum Hall effect

At fractional fillings of a Landau level, r_s is effectively ∞: A landau level is a massively degenerate flat band of single-particle states.

Naively, one would expect a Wigner crystal (or more exotic ground states with broken symmetry) to be selected by the interaction out of all possible degenerate Slater determinants.

Instead, for "magic" filling fractions, featureless (i.e., liquid like) ground states are selected by the screened Coulomb interaction.

For example, whenever $1/\nu$ is an odd integer, the featureless ground state is an incompressible ground state called a Laughlin state.

The fractional quantum Hall effect

At fractional fillings of a Landau level, r_s is effectively ∞: A landau level is a massively degenerate flat band of single-particle states.

Naively, one would expect a Wigner crystal (or more exotic ground states with broken symmetry) to be selected by the interaction out of all possible degenerate Slater determinants.

Instead, for “magic” filling fractions, featureless (i.e., liquid like) ground states are selected by the screened Coulomb interaction.

For example, whenever $1/\nu$ is an odd integer, the featureless ground state is an incompressible ground state called a Laughlin state.

Distinctive signature

The conductivity tensor is given by the classical Drude formula

$$\lim_{\tau\to\infty} \boldsymbol{j} = \begin{pmatrix} 0 & +\left(BR_{\mathrm{H}}\right)^{-1} \\ -\left(BR_{\mathrm{H}}\right)^{-1} & 0 \end{pmatrix} \boldsymbol{E}, \qquad R_{\mathrm{H}}^{-1} := -n\,e\,c,$$

in the ballistic regime when translation invariance is not broken.

In the presence of moderate static disorder, all but one single-particles are localized in a Landau level whereas many-body groundstates such as the Wigner crystal are pinned.

In the presence of moderate static disorder the magic filling fractions turn into plateaus at which

$$\sigma_{xx} = 0, \qquad \sigma_{xy} = \nu \times \frac{e^2}{h}$$

as a function of B for fixed n.

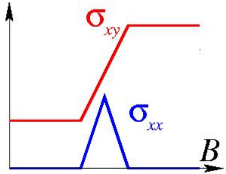

Distinctive signature

The conductivity tensor is given by the classical Drude formula

$$\lim_{\tau\to\infty} \boldsymbol{j} = \begin{pmatrix} 0 & +\left(BR_{\mathrm{H}}\right)^{-1} \\ -\left(BR_{\mathrm{H}}\right)^{-1} & 0 \end{pmatrix} \boldsymbol{E}, \qquad R_{\mathrm{H}}^{-1} := -n\,e\,c,$$

in the ballistic regime when translation invariance is not broken.

In the presence of moderate static disorder, all but one single-particles are localized in a Landau level whereas many-body groundstates such as the Wigner crystal are pinned.

In the presence of moderate static disorder the magic filling fractions turn into plateaus at which

$$\sigma_{xx} = 0, \qquad \sigma_{xy} = \nu \times \frac{e^2}{h}$$

as a function of B for fixed n.

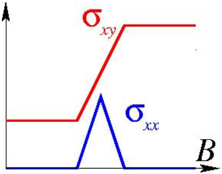

Distinctive signature

The conductivity tensor is given by the classical Drude formula

$$\lim_{\tau\to\infty} \boldsymbol{j} = \begin{pmatrix} 0 & +\left(BR_{\mathrm{H}}\right)^{-1} \\ -\left(BR_{\mathrm{H}}\right)^{-1} & 0 \end{pmatrix} \boldsymbol{E}, \qquad R_{\mathrm{H}}^{-1} := -n\,e\,c,$$

in the ballistic regime when translation invariance is not broken.

In the presence of moderate static disorder, all but one single-particles are localized in a Landau level whereas many-body groundstates such as the Wigner crystal are pinned.

In the presence of moderate static disorder the magic filling fractions turn into plateaus at which

$$\sigma_{xx} = 0, \qquad \sigma_{xy} = \nu \times \frac{e^2}{h}$$

as a function of B for fixed n.

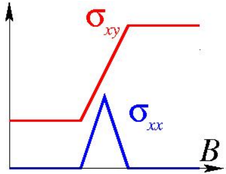

Strong interacting limit in lattice models

In any lattice model, the single-particle Bloch spectrum is bounded from above and from below.

The only possible way to take the ratio

$$r_{\mathrm{s}} := \frac{V_{\mathrm{int}}}{\Delta E_i} \to \infty$$

between the characteristic interaction energy scale V_{int} and the band width ΔE_i of the i-th Bloch band without inducing inter-band transitions to the bands $i-1$ and $i+1$ is to flatten the i-th Bloch band, $\Delta E_i \to 0$ while keeping the gaps to the $i-1$ and $i+1$ Bloch bands much larger than V_{int}.

Can band-flattening and interactions deliver a fractional quantum Hall state without an applied uniform magnetic field?

Strong interacting limit in lattice models

In any lattice model, the single-particle Bloch spectrum is bounded from above and from below.

The only possible way to take the ratio

$$r_{\mathrm{s}} := \frac{V_{\mathrm{int}}}{\Delta E_i} \to \infty$$

between the characteristic interaction energy scale V_{int} and the band width ΔE_i of the i-th Bloch band without inducing inter-band transitions to the bands $i-1$ and $i+1$ is to flatten the i-th Bloch band, $\Delta E_i \to 0$ while keeping the gaps to the $i-1$ and $i+1$ Bloch bands much larger than V_{int}.

Can band-flattening and interactions deliver a fractional quantum Hall state without an applied uniform magnetic field?

Strong interacting limit in lattice models

In any lattice model, the single-particle Bloch spectrum is bounded from above and from below.

The only possible way to take the ratio

$$r_{\mathrm{s}} := \frac{V_{\mathrm{int}}}{\Delta E_i} \to \infty$$

between the characteristic interaction energy scale V_{int} and the band width ΔE_i of the i-th Bloch band without inducing inter-band transitions to the bands $i-1$ and $i+1$ is to flatten the i-th Bloch band, $\Delta E_i \to 0$ while keeping the gaps to the $i-1$ and $i+1$ Bloch bands much larger than V_{int}.

Can band-flattening and interactions deliver a fractional quantum Hall state without an applied uniform magnetic field?

Strong interacting limit in lattice models

In any lattice model, the single-particle Bloch spectrum is bounded from above and from below.

The only possible way to take the ratio

$$r_{\mathrm{s}} := \frac{V_{\mathrm{int}}}{\Delta E_i} \to \infty$$

between the characteristic interaction energy scale V_{int} and the band width ΔE_i of the i-th Bloch band without inducing inter-band transitions to the bands $i-1$ and $i+1$ is to flatten the i-th Bloch band, $\Delta E_i \to 0$ while keeping the gaps to the $i-1$ and $i+1$ Bloch bands much larger than V_{int}.

Can band-flattening and interactions deliver a fractional quantum Hall state without an applied uniform magnetic field?

Question: Can band-flattening and interactions deliver a fractional quantum Hall state without an applied uniform magnetic field?

- E. Tang, J. W. Mei, and X. G. Wen, Phys. Rev. Lett., **106**, 236802 (2011).
- K. Sun, Z. Gu, H. Katsura, and S. Das Sarma, Phys. Rev. Lett., **106**, 236803 (2011).
- T. Neupert, L. Santos, C. Chamon, and C. Mudry, Phys. Rev. Lett., **106**, 236803 (2011).

Numerical answer: Yes!

- T. Neupert, L. Santos, C. Chamon, and C. Mudry, Phys. Rev. Lett., **106**, 236803 (2011).
- D. N. Sheng, Z. Gu, K. Sun, and L. Sheng, arXiv:1102.2658.
- Y.-F. Wang, Z.-C. Gu, C.-D. Gong, D. N. Sheng, arXiv:1103.1686.
- N. Regnault and B. A. Bernevig, arXiv:1105.4867.
- T. Neupert, L. Santos, S. Ryu, C. Chamon, and C. Mudry, arXiv:1106.3989.
- D. Xiao, W. Zhu, Y. Ran, N. Nagaosa, and S. Okamoto, arXiv:1106.4296.

Question: Can band-flattening and interactions deliver a fractional quantum Hall state without an applied uniform magnetic field?

- E. Tang, J. W. Mei, and X. G. Wen, Phys. Rev. Lett., **106**, 236802 (2011).
- K. Sun, Z. Gu, H. Katsura, and S. Das Sarma, Phys. Rev. Lett., **106**, 236803 (2011).
- T. Neupert, L. Santos, C. Chamon, and C. Mudry, Phys. Rev. Lett., **106**, 236803 (2011).

Numerical answer: Yes!

- T. Neupert, L. Santos, C. Chamon, and C. Mudry, Phys. Rev. Lett., **106**, 236803 (2011).
- D. N. Sheng, Z. Gu, K. Sun, and L. Sheng, arXiv:1102.2658.
- Y.-F. Wang, Z.-C. Gu, C.-D. Gong, D. N. Sheng, arXiv:1103.1686.
- N. Regnault and B. A. Bernevig, arXiv:1105.4867.
- T. Neupert, L. Santos, S. Ryu, C. Chamon, and C. Mudry, arXiv:1106.3989.
- D. Xiao, W. Zhu, Y. Ran, N. Nagaosa, and S. Okamoto, arXiv:1106.4296.

Question: Can band-flattening and interactions deliver a fractional quantum Hall state without an applied uniform magnetic field?

- E. Tang, J. W. Mei, and X. G. Wen, Phys. Rev. Lett., **106**, 236802 (2011).
- K. Sun, Z. Gu, H. Katsura, and S. Das Sarma, Phys. Rev. Lett., **106**, 236803 (2011).
- T. Neupert, L. Santos, C. Chamon, and C. Mudry, Phys. Rev. Lett., **106**, 236803 (2011).

Numerical answer: Yes!

- T. Neupert, L. Santos, C. Chamon, and C. Mudry, Phys. Rev. Lett., **106**, 236803 (2011).
- D. N. Sheng, Z. Gu, K. Sun, and L. Sheng, arXiv:1102.2658.
- Y.-F. Wang, Z.-C. Gu, C.-D. Gong, D. N. Sheng, arXiv:1103.1686.
- N. Regnault and B. A. Bernevig, arXiv:1105.4867.
- T. Neupert, L. Santos, S. Ryu, C. Chamon, and C. Mudry, arXiv:1106.3989.
- D. Xiao, W. Zhu, Y. Ran, N. Nagaosa, and S. Okamoto, arXiv:1106.4296.

Analytical approaches: Wave functions

- B. A. Bernevig and S.-C. Zhang, Phys. Rev. Lett. **96**, 106802 (2006).
- X.-L. Qi, arXiv:1105.4298.
- L. Santos, T. Neupert, S. Ryu, C. Chamon, and C. Mudry, arXiv:1108.2440.
- Yuan-Ming Lu and Ying Ran, arXiv:1109.0226.

Analytical approaches: Algebraic

- S. Parameswaran, R. Roy, and S. Sondhi, arXiv:1106.4025.
- M. O. Goerbig, arXiv:1107.1986.
- G. Murthy and R. Shankar, arXiv:1108.5501.

Analytical approaches: Effective quantum field theories for time-reversal symmetric fractional topological insulators

- M. Levin and A. Stern, Phys. Rev. Lett. **103**, 196803 (2009).
- T. Neupert, L. Santos, S. Ryu, C. Chamon, and C. Mudry, arXiv:1106.3989.
- L. Santos, T. Neupert, S. Ryu, C. Chamon, and C. Mudry, arXiv:1108.2440.
- Yuan-Ming Lu and Ying Ran, arXiv:1109.0226.

Analytical approaches: Wave functions

- B. A. Bernevig and S.-C. Zhang, Phys. Rev. Lett. **96**, 106802 (2006).
- X.-L. Qi, arXiv:1105.4298.
- L. Santos, T. Neupert, S. Ryu, C. Chamon, and C. Mudry, arXiv:1108.2440.
- Yuan-Ming Lu and Ying Ran, arXiv:1109.0226.

Analytical approaches: Algebraic

- S. Parameswaran, R. Roy, and S. Sondhi, arXiv:1106.4025.
- M. O. Goerbig, arXiv:1107.1986.
- G. Murthy and R. Shankar, arXiv:1108.5501.

Analytical approaches: Effective quantum field theories for time-reversal symmetric fractional topological insulators

- M. Levin and A. Stern, Phys. Rev. Lett. **103**, 196803 (2009).
- T. Neupert, L. Santos, S. Ryu, C. Chamon, and C. Mudry, arXiv:1106.3989.
- L. Santos, T. Neupert, S. Ryu, C. Chamon, and C. Mudry, arXiv:1108.2440.
- Yuan-Ming Lu and Ying Ran, arXiv:1109.0226.

Analytical approaches: Wave functions

- B. A. Bernevig and S.-C. Zhang, Phys. Rev. Lett. **96**, 106802 (2006).
- X.-L. Qi, arXiv:1105.4298.
- L. Santos, T. Neupert, S. Ryu, C. Chamon, and C. Mudry, arXiv:1108.2440.
- Yuan-Ming Lu and Ying Ran, arXiv:1109.0226.

Analytical approaches: Algebraic

- S. Parameswaran, R. Roy, and S. Sondhi, arXiv:1106.4025.
- M. O. Goerbig, arXiv:1107.1986.
- G. Murthy and R. Shankar, arXiv:1108.5501.

Analytical approaches: Effective quantum field theories for time-reversal symmetric fractional topological insulators

- M. Levin and A. Stern, Phys. Rev. Lett. **103**, 196803 (2009).
- T. Neupert, L. Santos, S. Ryu, C. Chamon, and C. Mudry, arXiv:1106.3989.
- L. Santos, T. Neupert, S. Ryu, C. Chamon, and C. Mudry, arXiv:1108.2440.
- Yuan-Ming Lu and Ying Ran, arXiv:1109.0226.

Analytical approaches: Wave functions

- B. A. Bernevig and S.-C. Zhang, Phys. Rev. Lett. **96**, 106802 (2006).
- X.-L. Qi, arXiv:1105.4298.
- L. Santos, T. Neupert, S. Ryu, C. Chamon, and C. Mudry, arXiv:1108.2440.
- Yuan-Ming Lu and Ying Ran, arXiv:1109.0226.

Analytical approaches: Algebraic

- S. Parameswaran, R. Roy, and S. Sondhi, arXiv:1106.4025.
- M. O. Goerbig, arXiv:1107.1986.
- G. Murthy and R. Shankar, arXiv:1108.5501.

Analytical approaches: Effective quantum field theories for time-reversal symmetric fractional topological insulators

- M. Levin and A. Stern, Phys. Rev. Lett. **103**, 196803 (2009).
- T. Neupert, L. Santos, S. Ryu, C. Chamon, and C. Mudry, arXiv:1106.3989.
- L. Santos, T. Neupert, S. Ryu, C. Chamon, and C. Mudry, arXiv:1108.2440.
- Yuan-Ming Lu and Ying Ran, arXiv:1109.0226.

Definition of the noninteracting lattice models

Let $\Lambda = \mathrm{A} \cup \mathrm{B}$ be a bipartite 2-dimensional lattice.

Example 1: Honeycomb lattice

Example 2: Square lattice

If spinless electrons are hopping so as to preserve the point group sublattice symmetry of sublattice A, then

$$H_0 := \sum_{\boldsymbol{k}\in\mathrm{BZ}} \psi^{\dagger}_{\boldsymbol{k}} \mathcal{H}_{\boldsymbol{k}} \psi_{\boldsymbol{k}}, \qquad \mathcal{H}_{\boldsymbol{k}} := B_{0,\boldsymbol{k}}\sigma_0 + \boldsymbol{B}_{\boldsymbol{k}} \cdot \boldsymbol{\sigma}, \qquad \psi_{\boldsymbol{k}} := \begin{pmatrix} c_{\boldsymbol{k},\mathrm{A}} \\ c_{\boldsymbol{k},\mathrm{B}} \end{pmatrix}$$

where BZ stands for the Brillouin zone of the A sublattice.

Definition of the noninteracting lattice models

Let $\Lambda = \mathrm{A} \cup \mathrm{B}$ be a bipartite 2-dimensional lattice.

Example 1: Honeycomb lattice

Example 2: Square lattice

If spinless electrons are hopping so as to preserve the point group sublattice symmetry of sublattice A, then

$$H_0 := \sum_{\boldsymbol{k}\in \mathrm{BZ}} \psi^\dagger_{\boldsymbol{k}} \mathcal{H}_{\boldsymbol{k}} \psi_{\boldsymbol{k}}, \qquad \mathcal{H}_{\boldsymbol{k}} := B_{0,\boldsymbol{k}}\sigma_0 + \boldsymbol{B}_{\boldsymbol{k}} \cdot \boldsymbol{\sigma}, \qquad \psi_{\boldsymbol{k}} := \begin{pmatrix} c_{\boldsymbol{k},\mathrm{A}} \\ c_{\boldsymbol{k},\mathrm{B}} \end{pmatrix}$$

where BZ stands for the Brillouin zone of the A sublattice.

Definition of the noninteracting lattice models

Let $\Lambda = \mathrm{A} \cup \mathrm{B}$ be a bipartite 2-dimensional lattice.

Example 1: Honeycomb lattice

Example 2: Square lattice

If spinless electrons are hopping so as to preserve the point group sublattice symmetry of sublattice A, then

$$H_0 := \sum_{\boldsymbol{k} \in \mathrm{BZ}} \psi^\dagger_{\boldsymbol{k}} \mathcal{H}_{\boldsymbol{k}} \psi_{\boldsymbol{k}}, \qquad \mathcal{H}_{\boldsymbol{k}} := B_{0,\boldsymbol{k}} \sigma_0 + \boldsymbol{B}_{\boldsymbol{k}} \cdot \boldsymbol{\sigma}, \qquad \psi_{\boldsymbol{k}} := \begin{pmatrix} c_{\boldsymbol{k},\mathrm{A}} \\ c_{\boldsymbol{k},\mathrm{B}} \end{pmatrix}$$

where BZ stands for the Brillouin zone of the A sublattice.

Definition of the noninteracting lattice models

Let $\Lambda = \mathrm{A} \cup \mathrm{B}$ be a bipartite 2-dimensional lattice.

Example 1: Honeycomb lattice

Example 2: Square lattice

If spinless electrons are hopping so as to preserve the point group sublattice symmetry of sublattice A, then

$$H_0 := \sum_{\boldsymbol{k}\in\mathrm{BZ}} \psi^{\dagger}_{\boldsymbol{k}} \mathcal{H}_{\boldsymbol{k}} \psi_{\boldsymbol{k}}, \qquad \mathcal{H}_{\boldsymbol{k}} := B_{0,\boldsymbol{k}}\sigma_0 + \boldsymbol{B}_{\boldsymbol{k}} \cdot \boldsymbol{\sigma}, \qquad \psi_{\boldsymbol{k}} := \begin{pmatrix} c_{\boldsymbol{k},\mathrm{A}} \\ c_{\boldsymbol{k},\mathrm{B}} \end{pmatrix}$$

where BZ stands for the Brillouin zone of the A sublattice.

Chern numbers

If we define

$$\widehat{\boldsymbol{B}}_{\boldsymbol{k}} := \frac{\boldsymbol{B}_{\boldsymbol{k}}}{|\boldsymbol{B}_{\boldsymbol{k}}|}, \quad \tan\phi_{\boldsymbol{k}} := \frac{\widehat{B}_{2,\boldsymbol{k}}}{\widehat{B}_{1,\boldsymbol{k}}}, \quad \cos\theta_{\boldsymbol{k}} := \widehat{B}_{3,\boldsymbol{k}},$$

then eigenvalues and eigenvectors of Hamiltonian $\mathcal{H}_{\boldsymbol{k}}$ are

$$\varepsilon_{\pm,\boldsymbol{k}} = B_{0,\boldsymbol{k}} \pm |\boldsymbol{B}_{\boldsymbol{k}}|, \quad \chi_{+,\boldsymbol{k}} = \begin{pmatrix} e^{-\mathrm{i}\phi_{\boldsymbol{k}}/2}\cos\frac{\theta_{\boldsymbol{k}}}{2} \\ e^{+\mathrm{i}\phi_{\boldsymbol{k}}/2}\sin\frac{\theta_{\boldsymbol{k}}}{2} \end{pmatrix}, \quad \chi_{-,\boldsymbol{k}} = \begin{pmatrix} e^{-\mathrm{i}\phi_{\boldsymbol{k}}/2}\sin\frac{\theta_{\boldsymbol{k}}}{2} \\ -e^{+\mathrm{i}\phi_{\boldsymbol{k}}/2}\cos\frac{\theta_{\boldsymbol{k}}}{2} \end{pmatrix}.$$

The first Chern-numbers for the bands labeled by $\pm$ are

$$C_{\pm} = \mp \int\limits_{\boldsymbol{k}\in\mathrm{BZ}} \frac{\mathrm{d}^2\boldsymbol{k}}{4\pi}\, \epsilon_{\mu\nu} \left[\partial_{k_\mu} \cos\theta(\boldsymbol{k})\right] \left[\partial_{k_\nu} \phi(\boldsymbol{k})\right].$$

They have opposite signs if non-zero. All the information about the topology of the Bloch bands of a gaped system is encoded in the occupied single-particle Bloch wave functions.

Chern numbers

If we define

$$\widehat{\boldsymbol{B}}_{\boldsymbol{k}} := \frac{\boldsymbol{B}_{\boldsymbol{k}}}{|\boldsymbol{B}_{\boldsymbol{k}}|}, \quad \tan\phi_{\boldsymbol{k}} := \frac{\widehat{B}_{2,\boldsymbol{k}}}{\widehat{B}_{1,\boldsymbol{k}}}, \quad \cos\theta_{\boldsymbol{k}} := \widehat{B}_{3,\boldsymbol{k}},$$

then eigenvalues and eigenvectors of Hamiltonian $\mathcal{H}_{\boldsymbol{k}}$ are

$$\varepsilon_{\pm,\boldsymbol{k}} = B_{0,\boldsymbol{k}} \pm |\boldsymbol{B}_{\boldsymbol{k}}|, \quad \chi_{+,\boldsymbol{k}} = \begin{pmatrix} e^{-\mathrm{i}\phi_{\boldsymbol{k}}/2}\cos\frac{\theta_{\boldsymbol{k}}}{2} \\ e^{+\mathrm{i}\phi_{\boldsymbol{k}}/2}\sin\frac{\theta_{\boldsymbol{k}}}{2} \end{pmatrix}, \quad \chi_{-,\boldsymbol{k}} = \begin{pmatrix} e^{-\mathrm{i}\phi_{\boldsymbol{k}}/2}\sin\frac{\theta_{\boldsymbol{k}}}{2} \\ -e^{+\mathrm{i}\phi_{\boldsymbol{k}}/2}\cos\frac{\theta_{\boldsymbol{k}}}{2} \end{pmatrix}.$$

The first Chern-numbers for the bands labeled by $\pm$ are

$$C_{\pm} = \mp \int\limits_{\boldsymbol{k}\in\mathrm{BZ}} \frac{\mathrm{d}^2\boldsymbol{k}}{4\pi}\, \epsilon_{\mu\nu} \left[\partial_{k_\mu}\cos\theta(\boldsymbol{k})\right]\left[\partial_{k_\nu}\phi(\boldsymbol{k})\right].$$

They have opposite signs if non-zero. All the information about the topology of the Bloch bands of a gaped system is encoded in the occupied single-particle Bloch wave functions.

Chern numbers

If we define

$$\widehat{\boldsymbol{B}}_{\boldsymbol{k}} := \frac{\boldsymbol{B}_{\boldsymbol{k}}}{|\boldsymbol{B}_{\boldsymbol{k}}|}, \quad \tan\phi_{\boldsymbol{k}} := \frac{\widehat{B}_{2,\boldsymbol{k}}}{\widehat{B}_{1,\boldsymbol{k}}}, \quad \cos\theta_{\boldsymbol{k}} := \widehat{B}_{3,\boldsymbol{k}},$$

then eigenvalues and eigenvectors of Hamiltonian $\mathcal{H}_{\boldsymbol{k}}$ are

$$\varepsilon_{\pm,\boldsymbol{k}} = B_{0,\boldsymbol{k}} \pm |\boldsymbol{B}_{\boldsymbol{k}}|, \quad \chi_{+,\boldsymbol{k}} = \begin{pmatrix} e^{-\mathrm{i}\phi_{\boldsymbol{k}}/2}\cos\frac{\theta_{\boldsymbol{k}}}{2} \\ e^{+\mathrm{i}\phi_{\boldsymbol{k}}/2}\sin\frac{\theta_{\boldsymbol{k}}}{2} \end{pmatrix}, \quad \chi_{-,\boldsymbol{k}} = \begin{pmatrix} e^{-\mathrm{i}\phi_{\boldsymbol{k}}/2}\sin\frac{\theta_{\boldsymbol{k}}}{2} \\ -e^{+\mathrm{i}\phi_{\boldsymbol{k}}/2}\cos\frac{\theta_{\boldsymbol{k}}}{2} \end{pmatrix}.$$

The first Chern-numbers for the bands labeled by $\pm$ are

$$C_{\pm} = \mp \int\limits_{\boldsymbol{k}\in\mathrm{BZ}} \frac{\mathrm{d}^2\boldsymbol{k}}{4\pi}\,\epsilon_{\mu\nu}\left[\partial_{k_\mu}\cos\theta(\boldsymbol{k})\right]\left[\partial_{k_\nu}\phi(\boldsymbol{k})\right].$$

They have opposite signs if non-zero. All the information about the topology of the Bloch bands of a gaped system is encoded in the occupied single-particle Bloch wave functions.

Chern numbers

If we define

$$\widehat{\boldsymbol{B}}_{\boldsymbol{k}} := \frac{\boldsymbol{B}_{\boldsymbol{k}}}{|\boldsymbol{B}_{\boldsymbol{k}}|}, \quad \tan\phi_{\boldsymbol{k}} := \frac{\widehat{B}_{2,\boldsymbol{k}}}{\widehat{B}_{1,\boldsymbol{k}}}, \quad \cos\theta_{\boldsymbol{k}} := \widehat{B}_{3,\boldsymbol{k}},$$

then eigenvalues and eigenvectors of Hamiltonian $\mathcal{H}_{\boldsymbol{k}}$ are

$$\varepsilon_{\pm,\boldsymbol{k}} = B_{0,\boldsymbol{k}} \pm |\boldsymbol{B}_{\boldsymbol{k}}|, \quad \chi_{+,\boldsymbol{k}} = \begin{pmatrix} e^{-\mathrm{i}\phi_{\boldsymbol{k}}/2}\cos\frac{\theta_{\boldsymbol{k}}}{2} \\ e^{+\mathrm{i}\phi_{\boldsymbol{k}}/2}\sin\frac{\theta_{\boldsymbol{k}}}{2} \end{pmatrix}, \quad \chi_{-,\boldsymbol{k}} = \begin{pmatrix} e^{-\mathrm{i}\phi_{\boldsymbol{k}}/2}\sin\frac{\theta_{\boldsymbol{k}}}{2} \\ -e^{+\mathrm{i}\phi_{\boldsymbol{k}}/2}\cos\frac{\theta_{\boldsymbol{k}}}{2} \end{pmatrix}.$$

The first Chern-numbers for the bands labeled by $\pm$ are

$$C_{\pm} = \mp \int\limits_{\boldsymbol{k}\in\mathrm{BZ}} \frac{\mathrm{d}^2\boldsymbol{k}}{4\pi}\, \epsilon_{\mu\nu} \left[\partial_{k_\mu} \cos\theta(\boldsymbol{k})\right] \left[\partial_{k_\nu} \phi(\boldsymbol{k})\right].$$

They have opposite signs if non-zero. All the information about the topology of the Bloch bands of a gaped system is encoded in the occupied single-particle Bloch wave functions.

Chern numbers

If we define

$$\widehat{\boldsymbol{B}}_{\boldsymbol{k}} := \frac{\boldsymbol{B}_{\boldsymbol{k}}}{|\boldsymbol{B}_{\boldsymbol{k}}|}, \quad \tan\phi_{\boldsymbol{k}} := \frac{\widehat{B}_{2,\boldsymbol{k}}}{\widehat{B}_{1,\boldsymbol{k}}}, \quad \cos\theta_{\boldsymbol{k}} := \widehat{B}_{3,\boldsymbol{k}},$$

then eigenvalues and eigenvectors of Hamiltonian $\mathcal{H}_{\boldsymbol{k}}$ are

$$\varepsilon_{\pm,\boldsymbol{k}} = B_{0,\boldsymbol{k}} \pm |\boldsymbol{B}_{\boldsymbol{k}}|, \quad \chi_{+,\boldsymbol{k}} = \begin{pmatrix} e^{-\mathrm{i}\phi_{\boldsymbol{k}}/2}\cos\frac{\theta_{\boldsymbol{k}}}{2} \\ e^{+\mathrm{i}\phi_{\boldsymbol{k}}/2}\sin\frac{\theta_{\boldsymbol{k}}}{2} \end{pmatrix}, \quad \chi_{-,\boldsymbol{k}} = \begin{pmatrix} e^{-\mathrm{i}\phi_{\boldsymbol{k}}/2}\sin\frac{\theta_{\boldsymbol{k}}}{2} \\ -e^{+\mathrm{i}\phi_{\boldsymbol{k}}/2}\cos\frac{\theta_{\boldsymbol{k}}}{2} \end{pmatrix}.$$

The first Chern-numbers for the bands labeled by $\pm$ are

$$C_{\pm} = \mp \int\limits_{\boldsymbol{k}\in\mathrm{BZ}} \frac{\mathrm{d}^2\boldsymbol{k}}{4\pi}\, \epsilon_{\mu\nu} \left[\partial_{k_\mu} \cos\theta(\boldsymbol{k})\right] \left[\partial_{k_\nu} \phi(\boldsymbol{k})\right].$$

They have opposite signs if non-zero. All the information about the topology of the Bloch bands of a gaped system is encoded in the occupied single-particle Bloch wave functions.

Example 1: Honeycomb lattice (Haldane 1988)

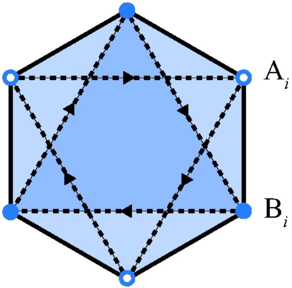

If the NN hopping amplitude, $t_1 > 0$, is positive (solid lines) and the NNN hopping amplitude are $t_2 e^{i2\pi\Phi/\Phi_0}$, with $t_2 \geq 0$, in the direction of the arrow (dotted lines),

then

$$B_{0,\boldsymbol{k}} := 2t_2 \cos\Phi \sum_{i=1}^{3} \cos \boldsymbol{k}\cdot\boldsymbol{b}_i,$$

$$\boldsymbol{B}_{\boldsymbol{k}} := \sum_{i=1}^{3} \begin{pmatrix} t_1 \cos \boldsymbol{k}\cdot\boldsymbol{a}_i \\ t_1 \sin \boldsymbol{k}\cdot\boldsymbol{a}_i \\ -2t_2 \sin\Phi \sin \boldsymbol{k}\cdot\boldsymbol{b}_i \end{pmatrix}$$

($\cos\Phi = t_1/(4t_2) = 3\sqrt{3/43}$ with the lower-band flatness ratio 1/7)

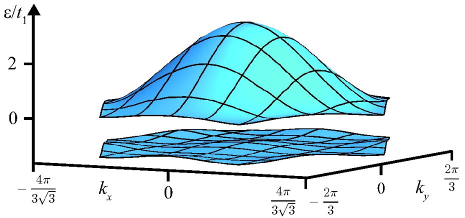

Example 1: Honeycomb lattice (Haldane 1988)

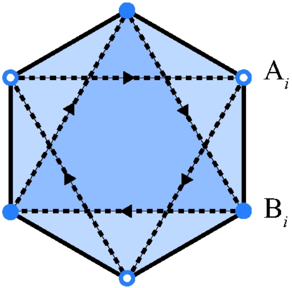

If the NN hopping amplitude, $t_1 > 0$, is positive (solid lines) and the NNN hopping amplitude are $t_2 e^{i2\pi\Phi/\Phi_0}$, with $t_2 \geq 0$, in the direction of the arrow (dotted lines),

then

$$B_{0,\boldsymbol{k}} := 2t_2 \cos\Phi \sum_{i=1}^{3} \cos \boldsymbol{k}\cdot\boldsymbol{b}_i,$$

$$\boldsymbol{B}_{\boldsymbol{k}} := \sum_{i=1}^{3} \begin{pmatrix} t_1 \cos \boldsymbol{k}\cdot\boldsymbol{a}_i \\ t_1 \sin \boldsymbol{k}\cdot\boldsymbol{a}_i \\ -2t_2 \sin\Phi \sin \boldsymbol{k}\cdot\boldsymbol{b}_i \end{pmatrix}$$

($\cos\Phi = t_1/(4t_2) = 3\sqrt{3/43}$ with the lower-band flatness ratio 1/7)

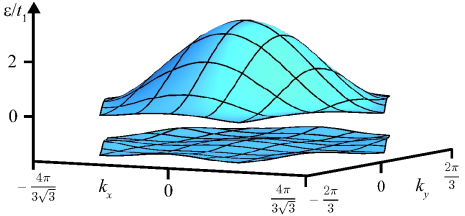

Example 1: Honeycomb lattice (Haldane 1988)

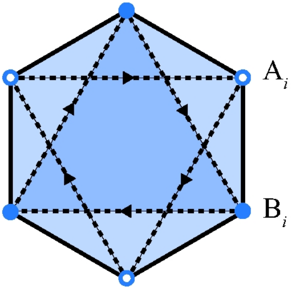

If the NN hopping amplitude, $t_1 > 0$, is positive (solid lines) and the NNN hopping amplitude are $t_2 e^{\mathrm{i}2\pi\Phi/\Phi_0}$, with $t_2 \geq 0$, in the direction of the arrow (dotted lines),

then

$$B_{0,\boldsymbol{k}} := 2t_2 \cos\Phi \sum_{i=1}^{3} \cos \boldsymbol{k}\cdot\boldsymbol{b}_i,$$

$$\boldsymbol{B}_{\boldsymbol{k}} := \sum_{i=1}^{3} \begin{pmatrix} t_1 \cos \boldsymbol{k}\cdot\boldsymbol{a}_i \\ t_1 \sin \boldsymbol{k}\cdot\boldsymbol{a}_i \\ -2t_2 \sin\Phi \sin \boldsymbol{k}\cdot\boldsymbol{b}_i \end{pmatrix}$$

($\cos\Phi = t_1/(4t_2) = 3\sqrt{3/43}$ with the lower-band flatness ratio 1/7)

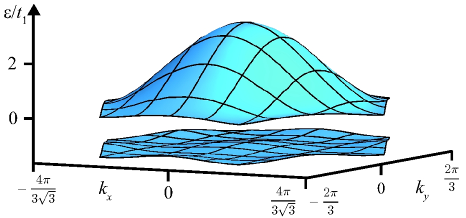

Example 1: Honeycomb lattice (Haldane 1988)

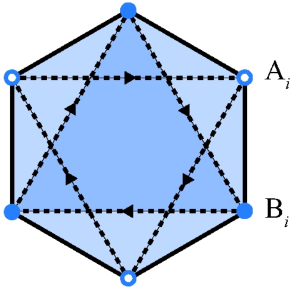

If the NN hopping amplitude, $t_1 > 0$, is positive (solid lines) and the NNN hopping amplitude are $t_2 e^{i2\pi\Phi/\Phi_0}$, with $t_2 \geq 0$, in the direction of the arrow (dotted lines),

then

$(\cos\Phi = t_1/(4t_2) = 3\sqrt{3/43}$ with the lower-band flatness ratio 1/7)

$$B_{0,\boldsymbol{k}} := 2t_2 \cos\Phi \sum_{i=1}^{3} \cos \boldsymbol{k}\cdot\boldsymbol{b_i},$$

$$\boldsymbol{B_k} := \sum_{i=1}^{3} \begin{pmatrix} t_1 \cos \boldsymbol{k}\cdot\boldsymbol{a_i} \\ t_1 \sin \boldsymbol{k}\cdot\boldsymbol{a_i} \\ -2t_2 \sin\Phi \sin \boldsymbol{k}\cdot\boldsymbol{b_i} \end{pmatrix}$$

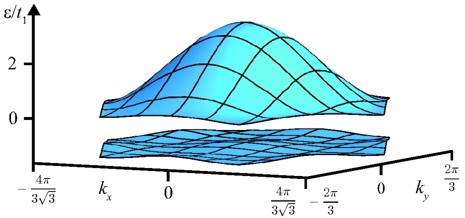

Example 2: Square lattice (Wen, Wilczek, and Zee 1989)

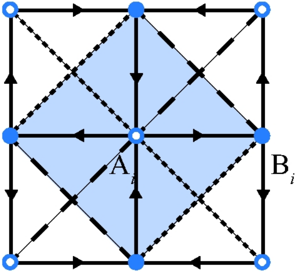

If the NN hopping amplitudes are $t_1 e^{i\pi/4}$, with $t_1 > 0$, in the direction of the arrow (solid lines) and the NNN hopping amplitudes are $t_2 \geq 0$ and $-t_2$ along the dashed and dotted lines, respectively.

then

$$B_{0,\boldsymbol{k}} := 0,$$

$$B_{1,\boldsymbol{k}} + iB_{2,\boldsymbol{k}} := t_1\, e^{-i\pi/4}\left[1+ e^{+i\left(k_y-k_x\right)}\right] + t_1\, e^{+i\pi/4}\left[e^{-ik_x} + e^{+ik_y}\right],$$

$$B_{3,\boldsymbol{k}} := 2t_2\left(\cos k_x - \cos k_y\right),$$

($t_1/t_2 = \sqrt{2}$ with the flatness ratio 1/5)

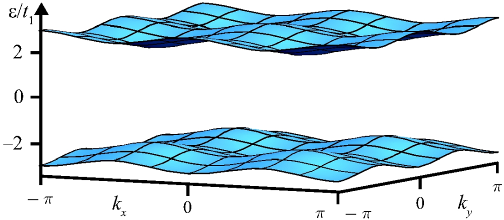

Example 2: Square lattice (Wen, Wilczek, and Zee 1989)

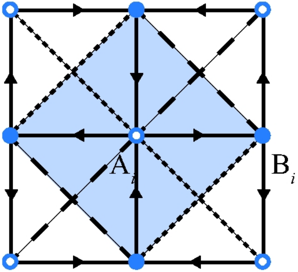

If the NN hopping amplitudes are $t_1\,e^{\mathrm{i}\pi/4}$, with $t_1 > 0$, in the direction of the arrow (solid lines) and the NNN hopping amplitudes are $t_2 \geq 0$ and $-t_2$ along the dashed and dotted lines, respectively.

then

$(t_1/t_2 = \sqrt{2}$ with the flatness ratio 1/5)

$$B_{0,\boldsymbol{k}} := 0,$$

$$B_{1,\boldsymbol{k}} + \mathrm{i}B_{2,\boldsymbol{k}} := t_1\,e^{-\mathrm{i}\pi/4}\left[1 + e^{+\mathrm{i}\left(k_y - k_x\right)}\right] + t_1\,e^{+\mathrm{i}\pi/4}\left[e^{-\mathrm{i}k_x} + e^{+\mathrm{i}k_y}\right],$$

$$B_{3,\boldsymbol{k}} := 2t_2\left(\cos k_x - \cos k_y\right),$$

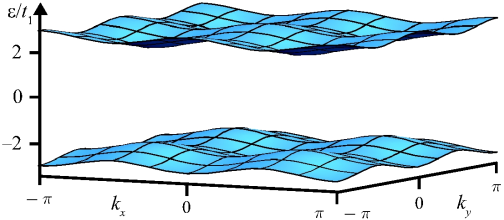

Example 2: Square lattice (Wen, Wilczek, and Zee 1989)

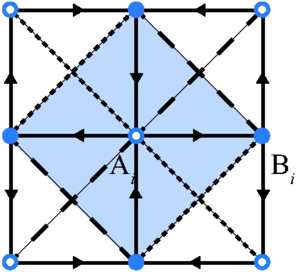

If the NN hopping amplitudes are $t_1\, e^{i\pi/4}$, with $t_1 > 0$, in the direction of the arrow (solid lines) and the NNN hopping amplitudes are $t_2 \geq 0$ and $-t_2$ along the dashed and dotted lines, respectively.

then

$(t_1/t_2 = \sqrt{2}$ with the flatness ratio 1/5)

$B_{0,\boldsymbol{k}} := 0,$

$B_{1,\boldsymbol{k}} + iB_{2,\boldsymbol{k}} := t_1\, e^{-i\pi/4}\left[1 + e^{+i(k_y - k_x)}\right] + t_1\, e^{+i\pi/4}\left[e^{-ik_x} + e^{+ik_y}\right],$

$B_{3,\boldsymbol{k}} := 2t_2\left(\cos k_x - \cos k_y\right),$

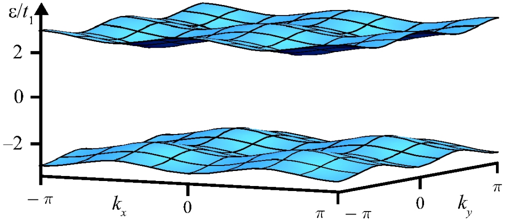

Example 2: Square lattice (Wen, Wilczek, and Zee 1989)

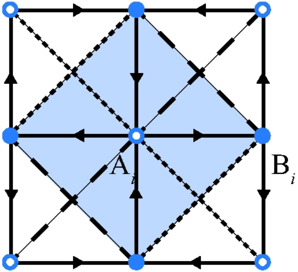

If the NN hopping amplitudes are $t_1 e^{\mathrm{i}\pi/4}$, with $t_1 > 0$, in the direction of the arrow (solid lines) and the NNN hopping amplitudes are $t_2 \geq 0$ and $-t_2$ along the dashed and dotted lines, respectively.

then

$$B_{0,\boldsymbol{k}} := 0,$$

$$B_{1,\boldsymbol{k}} + \mathrm{i}B_{2,\boldsymbol{k}} := t_1\, e^{-\mathrm{i}\pi/4}\left[1 + e^{+\mathrm{i}\left(k_y - k_x\right)}\right] + t_1\, e^{+\mathrm{i}\pi/4}\left[e^{-\mathrm{i}k_x} + e^{+\mathrm{i}k_y}\right],$$

$$B_{3,\boldsymbol{k}} := 2t_2\left(\cos k_x - \cos k_y\right),$$

($t_1/t_2 = \sqrt{2}$ with the flatness ratio 1/5)

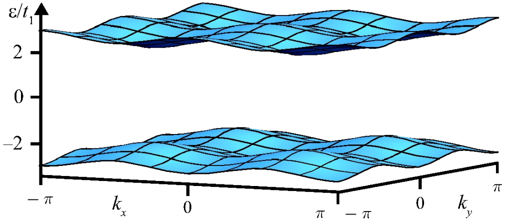

Band flattening

Band-flattening is defined by

$$\mathcal{H}^{\text{flat}}_{\boldsymbol{k}} := \frac{\mathcal{H}_{\boldsymbol{k}}}{\varepsilon_{-,\boldsymbol{k}}}.$$

Let there be N sites on sublattice A and N sites on sublattice B.

We fix the number of spinless fermions to be N (half-filled $\Lambda := \mathrm{A} \cup \mathrm{B}$).

Before band-flattening, the half-filled groundstate is

$$\langle \boldsymbol{r}_1, \cdots, \boldsymbol{r}_N | \boldsymbol{k}_1, \cdots, \boldsymbol{k}_N \rangle = \det \begin{pmatrix} e^{\mathrm{i}\boldsymbol{k}_1 \cdot \boldsymbol{r}_1} \chi_{-,\boldsymbol{k}_1} & \cdots & e^{\mathrm{i}\boldsymbol{k}_N \cdot \boldsymbol{r}_1} \chi_{-,\boldsymbol{k}_N} \\ \vdots & \vdots & \vdots \\ e^{\mathrm{i}\boldsymbol{k}_1 \cdot \boldsymbol{r}_N} \chi_{-,\boldsymbol{k}_1}, & \cdots & e^{\mathrm{i}\boldsymbol{k}_N \cdot \boldsymbol{r}_N} \chi_{-,\boldsymbol{k}_N} \end{pmatrix}.$$

After band-flattening, the half-filled groundstate has not changed, for all single-particle Bloch states are unchanged under band flattening.

Band flattening

Band-flattening is defined by

$$\mathcal{H}^{\text{flat}}_{\boldsymbol{k}} := \frac{\mathcal{H}_{\boldsymbol{k}}}{\varepsilon_{-,\boldsymbol{k}}}.$$

Let there be N sites on sublattice A and N sites on sublattice B.

We fix the number of spinless fermions to be N (half-filled $\Lambda := \mathrm{A} \cup \mathrm{B}$).

Before band-flattening, the half-filled groundstate is

$$\langle \boldsymbol{r}_1, \cdots, \boldsymbol{r}_N | \boldsymbol{k}_1, \cdots, \boldsymbol{k}_N \rangle = \det \begin{pmatrix} e^{\mathrm{i}\boldsymbol{k}_1 \cdot \boldsymbol{r}_1} \chi_{-,\boldsymbol{k}_1} & \cdots & e^{\mathrm{i}\boldsymbol{k}_N \cdot \boldsymbol{r}_1} \chi_{-,\boldsymbol{k}_N} \\ \vdots & \vdots & \vdots \\ e^{\mathrm{i}\boldsymbol{k}_1 \cdot \boldsymbol{r}_N} \chi_{-,\boldsymbol{k}_1}, & \cdots & e^{\mathrm{i}\boldsymbol{k}_N \cdot \boldsymbol{r}_N} \chi_{-,\boldsymbol{k}_N} \end{pmatrix}.$$

After band-flattening, the half-filled groundstate has not changed, for all single-particle Bloch states are unchanged under band flattening.

Band flattening

Band-flattening is defined by

$$\mathcal{H}^{\text{flat}}_{\boldsymbol{k}} := \frac{\mathcal{H}_{\boldsymbol{k}}}{\varepsilon_{-,\boldsymbol{k}}}.$$

Let there be N sites on sublattice A and N sites on sublattice B.

We fix the number of spinless fermions to be N (half-filled $\Lambda :=$ A $\cup$ B).

Before band-flattening, the half-filled groundstate is

$$\langle \boldsymbol{r}_1, \cdots, \boldsymbol{r}_N | \boldsymbol{k}_1, \cdots, \boldsymbol{k}_N \rangle = \det \begin{pmatrix} e^{\mathrm{i}\boldsymbol{k}_1\cdot\boldsymbol{r}_1}\chi_{-,\boldsymbol{k}_1} & \cdots & e^{\mathrm{i}\boldsymbol{k}_N\cdot\boldsymbol{r}_1}\chi_{-,\boldsymbol{k}_N} \\ \vdots & \vdots & \vdots \\ e^{\mathrm{i}\boldsymbol{k}_1\cdot\boldsymbol{r}_N}\chi_{-,\boldsymbol{k}_1}, & \cdots & e^{\mathrm{i}\boldsymbol{k}_N\cdot\boldsymbol{r}_N}\chi_{-,\boldsymbol{k}_N} \end{pmatrix}.$$

After band-flattening, the half-filled groundstate has not changed, for all single-particle Bloch states are unchanged under band flattening.

Band flattening

Band-flattening is defined by

$$\mathcal{H}^{\text{flat}}_{\boldsymbol{k}} := \frac{\mathcal{H}_{\boldsymbol{k}}}{\varepsilon_{-,\boldsymbol{k}}}.$$

Let there be N sites on sublattice A and N sites on sublattice B.

We fix the number of spinless fermions to be N (half-filled $\Lambda := \mathrm{A} \cup \mathrm{B}$).

Before band-flattening, the half-filled groundstate is

$$\langle \boldsymbol{r}_1, \cdots, \boldsymbol{r}_N | \boldsymbol{k}_1, \cdots, \boldsymbol{k}_N \rangle = \det \begin{pmatrix} e^{\mathrm{i}\boldsymbol{k}_1\cdot\boldsymbol{r}_1}\chi_{-,\boldsymbol{k}_1} & \cdots & e^{\mathrm{i}\boldsymbol{k}_N\cdot\boldsymbol{r}_1}\chi_{-,\boldsymbol{k}_N} \\ \vdots & \vdots & \vdots \\ e^{\mathrm{i}\boldsymbol{k}_1\cdot\boldsymbol{r}_N}\chi_{-,\boldsymbol{k}_1}, & \cdots & e^{\mathrm{i}\boldsymbol{k}_N\cdot\boldsymbol{r}_N}\chi_{-,\boldsymbol{k}_N} \end{pmatrix}.$$

After band-flattening, the half-filled groundstate has not changed, for all single-particle Bloch states are unchanged under band flattening.

Band flattening

Band-flattening is defined by

$$\mathcal{H}^{\text{flat}}_{\boldsymbol{k}} := \frac{\mathcal{H}_{\boldsymbol{k}}}{\varepsilon_{-,\boldsymbol{k}}}.$$

Let there be N sites on sublattice A and N sites on sublattice B.

We fix the number of spinless fermions to be N (half-filled $\Lambda := \text{A} \cup \text{B}$).

Before band-flattening, the half-filled groundstate is

$$\langle \boldsymbol{r}_1, \cdots, \boldsymbol{r}_N | \boldsymbol{k}_1, \cdots, \boldsymbol{k}_N \rangle = \det \begin{pmatrix} e^{\mathrm{i}\boldsymbol{k}_1 \cdot \boldsymbol{r}_1} \chi_{-,\boldsymbol{k}_1} & \cdots & e^{\mathrm{i}\boldsymbol{k}_N \cdot \boldsymbol{r}_1} \chi_{-,\boldsymbol{k}_N} \\ \vdots & \vdots & \vdots \\ e^{\mathrm{i}\boldsymbol{k}_1 \cdot \boldsymbol{r}_N} \chi_{-,\boldsymbol{k}_1}, & \cdots & e^{\mathrm{i}\boldsymbol{k}_N \cdot \boldsymbol{r}_N} \chi_{-,\boldsymbol{k}_N} \end{pmatrix}.$$

After band-flattening, the half-filled groundstate has not changed, for all single-particle Bloch states are unchanged under band flattening.

Band flattening

Band-flattening is defined by

$$\mathcal{H}^{\text{flat}}_{\boldsymbol{k}} := \frac{\mathcal{H}_{\boldsymbol{k}}}{\varepsilon_{-,\boldsymbol{k}}}.$$

Let there be N sites on sublattice A and N sites on sublattice B.

We fix the number of spinless fermions to be N (half-filled $\Lambda := \mathrm{A} \cup \mathrm{B}$).

Before band-flattening, the half-filled groundstate is

$$\langle \boldsymbol{r}_1, \cdots, \boldsymbol{r}_N | \boldsymbol{k}_1, \cdots, \boldsymbol{k}_N \rangle = \det \begin{pmatrix} e^{\mathrm{i}\boldsymbol{k}_1 \cdot \boldsymbol{r}_1} \chi_{-,\boldsymbol{k}_1} & \cdots & e^{\mathrm{i}\boldsymbol{k}_N \cdot \boldsymbol{r}_1} \chi_{-,\boldsymbol{k}_N} \\ \vdots & \vdots & \vdots \\ e^{\mathrm{i}\boldsymbol{k}_1 \cdot \boldsymbol{r}_N} \chi_{-,\boldsymbol{k}_1}, & \cdots & e^{\mathrm{i}\boldsymbol{k}_N \cdot \boldsymbol{r}_N} \chi_{-,\boldsymbol{k}_N} \end{pmatrix}.$$

After band-flattening, the half-filled groundstate has not changed, for all single-particle Bloch states are unchanged under band flattening.

Band flattening preserves locality

Let

$$\mathcal{O}_n(\boldsymbol{x}) := \sum_{i\in\Lambda} a_{n,i}\,\delta(\boldsymbol{x}-\boldsymbol{r}_i), \qquad n=1,2,$$

be any pair of two Hermitean local operators.

Define

$$C^{(1,2)}_{\boldsymbol{k}_1,\cdots,\boldsymbol{k}_N}(\boldsymbol{x},\boldsymbol{y}) := \langle \boldsymbol{k}_1,\cdots,\boldsymbol{k}_N\,|\mathcal{O}_1(\boldsymbol{x})\mathcal{O}_2(\boldsymbol{y})|\,\boldsymbol{k}_1,\cdots,\boldsymbol{k}_N\rangle\,.$$

The correlation function

$$C^{(1,2)}(\boldsymbol{x},\boldsymbol{y}) \propto e^{-\Delta|\boldsymbol{x}-\boldsymbol{y}|}$$

must decay exponentially before and after band flattening, for neither the existence of the single-particle gap Δ nor the eigenfunctions are affected by the band flattening.

Band flattening preserves locality

Let

$$\mathcal{O}_n(\boldsymbol{x}) := \sum_{i\in\Lambda} a_{n,i}\,\delta(\boldsymbol{x}-\boldsymbol{r}_i), \qquad n=1,2,$$

be any pair of two Hermitean local operators.

Define

$$C^{(1,2)}_{\boldsymbol{k}_1,\cdots,\boldsymbol{k}_N}(\boldsymbol{x},\boldsymbol{y}) := \langle \boldsymbol{k}_1,\cdots,\boldsymbol{k}_N|\mathcal{O}_1(\boldsymbol{x})\mathcal{O}_2(\boldsymbol{y})|\boldsymbol{k}_1,\cdots,\boldsymbol{k}_N\rangle\,.$$

The correlation function

$$C^{(1,2)}(\boldsymbol{x},\boldsymbol{y}) \propto e^{-\Delta|\boldsymbol{x}-\boldsymbol{y}|}$$

must decay exponentially before and after band flattening, for neither the existence of the single-particle gap Δ nor the eigenfunctions are affected by the band flattening.

Band flattening preserves locality

Let

$$\mathcal{O}_n(\boldsymbol{x}) := \sum_{i\in\Lambda} a_{n,i}\,\delta(\boldsymbol{x}-\boldsymbol{r}_i), \qquad n=1,2,$$

be any pair of two Hermitean local operators.

Define

$$C^{(1,2)}_{\boldsymbol{k}_1,\cdots,\boldsymbol{k}_N}(\boldsymbol{x},\boldsymbol{y}) := \langle \boldsymbol{k}_1,\cdots,\boldsymbol{k}_N\,|\mathcal{O}_1(\boldsymbol{x})\mathcal{O}_2(\boldsymbol{y})|\,\boldsymbol{k}_1,\cdots,\boldsymbol{k}_N\rangle\,.$$

The correlation function

$$C^{(1,2)}(\boldsymbol{x},\boldsymbol{y}) \propto e^{-\Delta|\boldsymbol{x}-\boldsymbol{y}|}$$

must decay exponentially before and after band flattening, for neither the existence of the single-particle gap Δ nor the eigenfunctions are affected by the band flattening.

Band flattening preserves locality

Let

$$\mathcal{O}_n(\boldsymbol{x}) := \sum_{i\in\Lambda} a_{n,i}\,\delta(\boldsymbol{x}-\boldsymbol{r}_i), \qquad n=1,2,$$

be any pair of two Hermitean local operators.

Define

$$C^{(1,2)}_{\boldsymbol{k}_1,\cdots,\boldsymbol{k}_N}(\boldsymbol{x},\boldsymbol{y}) := \langle \boldsymbol{k}_1,\cdots,\boldsymbol{k}_N|\mathcal{O}_1(\boldsymbol{x})\mathcal{O}_2(\boldsymbol{y})|\boldsymbol{k}_1,\cdots,\boldsymbol{k}_N\rangle\,.$$

The correlation function

$$C^{(1,2)}(\boldsymbol{x},\boldsymbol{y}) \propto e^{-\Delta|\boldsymbol{x}-\boldsymbol{y}|}$$

must decay exponentially before and after band flattening, for neither the existence of the single-particle gap Δ nor the eigenfunctions are affected by the band flattening.

Definition of the interacting lattice model

Define the many-body Hamiltonian

$$H := H_0^{\text{flat}} + H_{\text{int}}$$

where

$$H_{\text{int}} := \frac{1}{2}\sum_{i,j\in\Lambda} \rho_i V_{i,j} \rho_j \equiv V \sum_{\langle ij\rangle} \rho_i \rho_j, \qquad V>0,$$

and ρ_i is the occupation number on the site $i \in \Lambda := \text{A} \cup \text{B}$ of the square lattice.

Define the filling fraction ν to be the ratio

$$\nu := \frac{N_{\text{f}}}{N}$$

where N_{f} is the number of spinless fermions and N the number of sites in sublattice A of the square lattice.

Definition of the interacting lattice model

Define the many-body Hamiltonian

$$H := H_0^{\text{flat}} + H_{\text{int}}$$

where

$$H_{\text{int}} := \frac{1}{2} \sum_{i,j \in \Lambda} \rho_i V_{i,j} \rho_j \equiv V \sum_{\langle ij \rangle} \rho_i \rho_j, \qquad V > 0,$$

and ρ_i is the occupation number on the site $i \in \Lambda := \mathrm{A} \cup \mathrm{B}$ of the square lattice.

Define the filling fraction ν to be the ratio

$$\nu := \frac{N_{\mathrm{f}}}{N}$$

where N_{f} is the number of spinless fermions and N the number of sites in sublattice A of the square lattice.

Fractional quantum Hall ground state

Three distinctive properties of a fractional quantum Hall ground state at filling fraction $\nu < 1$ (where ν^{-1} is an odd integer) and with periodic boundary conditions (toroidal geometry) are

- the existence of a spectral gap above the ground state manifold,
- the ν^{-1}–fold topological degeneracy of the ground state manifold in the thermodynamic limit,
- and the quantization ν of the Hall conductance σ_{xy} in units of $\nu e^2/h$.

Fractional quantum Hall ground state

Three distinctive properties of a fractional quantum Hall ground state at filling fraction $\nu < 1$ (where ν^{-1} is an odd integer) and with periodic boundary conditions (toroidal geometry) are

- the existence of a spectral gap above the ground state manifold,
- the ν^{-1}–fold topological degeneracy of the ground state manifold in the thermodynamic limit,
- and the quantization ν of the Hall conductance σ_{xy} in units of $\nu e^2/h$.

Fractional quantum Hall ground state

Three distinctive properties of a fractional quantum Hall ground state at filling fraction $\nu < 1$ (where ν^{-1} is an odd integer) and with periodic boundary conditions (toroidal geometry) are

- the existence of a spectral gap above the ground state manifold,
- the ν^{-1}–fold topological degeneracy of the ground state manifold in the thermodynamic limit,
- and the quantization ν of the Hall conductance σ_{xy} in units of $\nu e^2/h$.

Fractional quantum Hall ground state

Three distinctive properties of a fractional quantum Hall ground state at filling fraction $\nu < 1$ (where ν^{-1} is an odd integer) and with periodic boundary conditions (toroidal geometry) are

- the existence of a spectral gap above the ground state manifold,
- the ν^{-1}–fold topological degeneracy of the ground state manifold in the thermodynamic limit,
- and the quantization ν of the Hall conductance σ_{xy} in units of $\nu e^2/h$.

Spectral gap if $N = 3 \times 6$ and $N_\mathrm{f} = 6$, i.e., $\nu = 1/3$

Add a sublattice-staggered chemical potential $4\mu_\mathrm{s}$ to the single-particle Hamiltonian by replacing $B_{3,\boldsymbol{k}} \to B_{3,\boldsymbol{k}} + 4\mu_\mathrm{s}$.

The parameters t_2 and μ_s of H_0^{flat} interpolate between topological ($|t_2| > |\mu_\mathrm{s}|$) and non-topological ($|t_2| < |\mu_\mathrm{s}|$) single-particle bands.

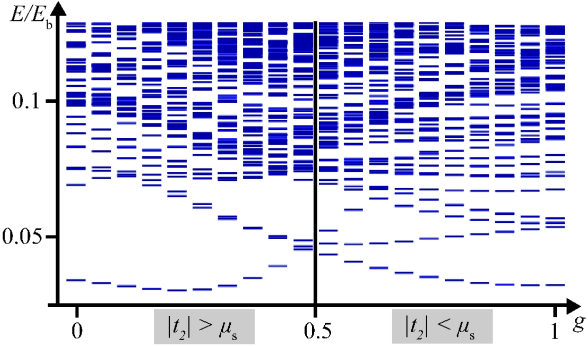

Here, $g := (2/\pi)\arctan|t_2/\mu_\mathrm{s}|$ and all energies are measured relative to the interacting band width E_b. The gap is of order V when $g = 0$.

Spectral gap if $N = 3 \times 6$ and $N_\mathrm{f} = 6$, i.e., $\nu = 1/3$

Add a sublattice-staggered chemical potential $4\mu_\mathrm{s}$ to the single-particle Hamiltonian by replacing $B_{3,\boldsymbol{k}} \to B_{3,\boldsymbol{k}} + 4\mu_\mathrm{s}$.

The parameters t_2 and μ_s of H_0^{flat} interpolate between topological ($|t_2| > |\mu_\mathrm{s}|$) and non-topological ($|t_2| < |\mu_\mathrm{s}|$) single-particle bands.

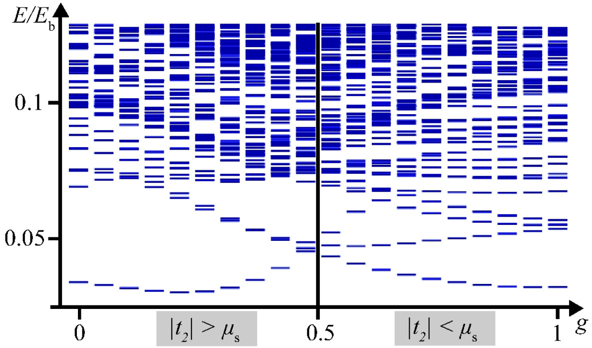

Here, $g := (2/\pi)\arctan|t_2/\mu_\mathrm{s}|$ and all energies are measured relative to the interacting band width E_b. The gap is of order V when $g = 0$.

Spectral gap if $N = 3 \times 6$ and $N_{\mathrm{f}} = 6$, i.e., $\nu = 1/3$

Add a sublattice-staggered chemical potential $4\mu_{\mathrm{s}}$ to the single-particle Hamiltonian by replacing $B_{3,\boldsymbol{k}} \to B_{3,\boldsymbol{k}} + 4\mu_{\mathrm{s}}$.

The parameters t_2 and μ_{s} of H_0^{flat} interpolate between topological ($|t_2| > |\mu_{\mathrm{s}}|$) and non-topological ($|t_2| < |\mu_{\mathrm{s}}|$) single-particle bands.

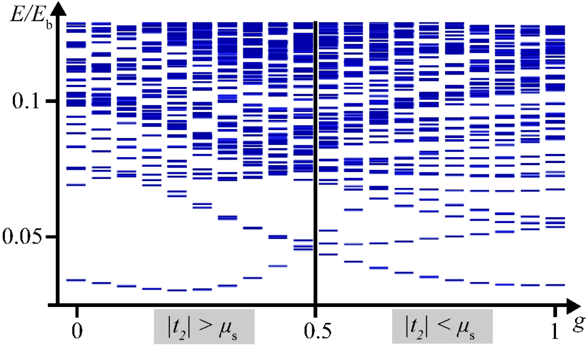

Here, $g := (2/\pi)\arctan|t_2/\mu_{\mathrm{s}}|$ and all energies are measured relative to the interacting band width E_b. The gap is of order V when $g = 0$.

Topological degeneracy if $N = 3 \times 6$ and $N_{\mathrm{f}} = 6$

Impose the twisted boundary conditions

$$|\Psi_\gamma(\boldsymbol{r} + N_x \boldsymbol{x})\rangle = e^{\mathrm{i}\gamma_x} |\Psi_\gamma(\boldsymbol{r})\rangle, \qquad |\Psi_\gamma(\boldsymbol{r} + N_y \boldsymbol{y})\rangle = e^{\mathrm{i}\gamma_y} |\Psi_\gamma(\boldsymbol{r})\rangle$$

where $\gamma^t = (\gamma_x, \gamma_y)$ are the twisting angles and $N_x \times N_y = N$ the number of unit cells.

Due to translational invariance, the Hamiltonian does not couple states with different center of mass momenta $\boldsymbol{Q} := \boldsymbol{k}_1 + \ldots + \boldsymbol{k}_{N_{\mathrm{f}}}$, where $\boldsymbol{k}_i$, $i = 1, \cdots, N_{\mathrm{f}}$ are the single-particle momenta of an N_{f}-particle state.

At 1/3 filling of the 3×6 sublattice A, the particle number $N_{\mathrm{f}} = 6$ is commensurate with the lattice dimensions and all three topological states have the same $\boldsymbol{Q}$.

As a consequence, their topological degeneracy is lifted and a unique ground state appears.

Topological degeneracy if $N = 3 \times 6$ and $N_{\mathrm{f}} = 6$

Impose the twisted boundary conditions

$$|\Psi_\gamma(\boldsymbol{r} + N_x \boldsymbol{x})\rangle = e^{\mathrm{i}\gamma_x} |\Psi_\gamma(\boldsymbol{r})\rangle, \qquad |\Psi_\gamma(\boldsymbol{r} + N_y \boldsymbol{y})\rangle = e^{\mathrm{i}\gamma_y} |\Psi_\gamma(\boldsymbol{r})\rangle$$

where $\gamma^t = (\gamma_x, \gamma_y)$ are the twisting angles and $N_x \times N_y = N$ the number of unit cells.

Due to translational invariance, the Hamiltonian does not couple states with different center of mass momenta $\boldsymbol{Q} := \boldsymbol{k}_1 + \ldots + \boldsymbol{k}_{N_{\mathrm{f}}}$, where $\boldsymbol{k}_i,\ i = 1, \cdots, N_{\mathrm{f}}$ are the single-particle momenta of an N_{f}-particle state.

At 1/3 filling of the 3×6 sublattice A, the particle number $N_{\mathrm{f}} = 6$ is commensurate with the lattice dimensions and all three topological states have the same $\boldsymbol{Q}$.

As a consequence, their topological degeneracy is lifted and a unique ground state appears.

Topological degeneracy if $N = 3 \times 6$ and $N_{\mathrm{f}} = 6$

Impose the twisted boundary conditions

$$|\Psi_\gamma(\boldsymbol{r} + N_x \boldsymbol{x})\rangle = e^{\mathrm{i}\gamma_x} |\Psi_\gamma(\boldsymbol{r})\rangle, \qquad |\Psi_\gamma(\boldsymbol{r} + N_y \boldsymbol{y})\rangle = e^{\mathrm{i}\gamma_y} |\Psi_\gamma(\boldsymbol{r})\rangle$$

where $\gamma^t = (\gamma_x, \gamma_y)$ are the twisting angles and $N_x \times N_y = N$ the number of unit cells.

Due to translational invariance, the Hamiltonian does not couple states with different center of mass momenta $\boldsymbol{Q} := \boldsymbol{k}_1 + \ldots + \boldsymbol{k}_{N_{\mathrm{f}}}$, where $\boldsymbol{k}_i,\ i = 1, \cdots, N_{\mathrm{f}}$ are the single-particle momenta of an N_{f}-particle state.

At 1/3 filling of the 3×6 sublattice A, the particle number $N_{\mathrm{f}} = 6$ is commensurate with the lattice dimensions and all three topological states have the same $\boldsymbol{Q}$.

As a consequence, their topological degeneracy is lifted and a unique ground state appears.

Topological degeneracy if $N = 3 \times 6$ and $N_{\mathrm{f}} = 6$

Impose the twisted boundary conditions

$$|\Psi_\gamma(\boldsymbol{r} + N_x \boldsymbol{x})\rangle = e^{\mathrm{i}\gamma_x} |\Psi_\gamma(\boldsymbol{r})\rangle, \qquad |\Psi_\gamma(\boldsymbol{r} + N_y \boldsymbol{y})\rangle = e^{\mathrm{i}\gamma_y} |\Psi_\gamma(\boldsymbol{r})\rangle$$

where $\gamma^t = (\gamma_x, \gamma_y)$ are the twisting angles and $N_x \times N_y = N$ the number of unit cells.

Due to translational invariance, the Hamiltonian does not couple states with different center of mass momenta $\boldsymbol{Q} := \boldsymbol{k}_1 + \ldots + \boldsymbol{k}_{N_{\mathrm{f}}}$, where $\boldsymbol{k}_i,\ i = 1, \cdots, N_{\mathrm{f}}$ are the single-particle momenta of an N_{f}-particle state.

At 1/3 filling of the 3×6 sublattice A, the particle number $N_{\mathrm{f}} = 6$ is commensurate with the lattice dimensions and all three topological states have the same $\boldsymbol{Q}$.

As a consequence, their topological degeneracy is lifted and a unique ground state appears.

We can now use twisted boundary conditions to probe the topological nature of the ground state: varying γ_x between 0 and 2π is equivalent to the adiabatic insertion of a flux quantum in the system.

During this process, a topological ground state with $\sigma_{xy} \times h/e^2 = 1/3$ should undergo two level crossings with the other two gaped topological states (Thouless 1989).

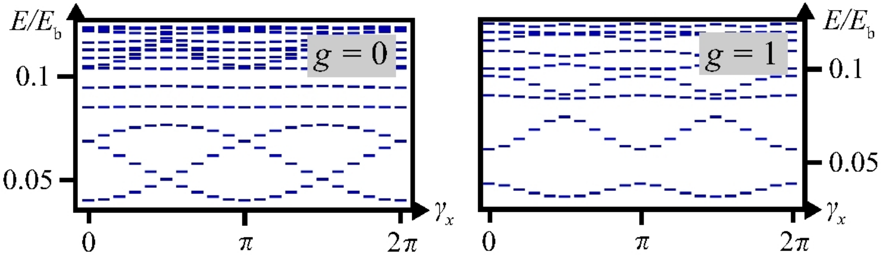

We can now use twisted boundary conditions to probe the topological nature of the ground state: varying γ_x between 0 and 2π is equivalent to the adiabatic insertion of a flux quantum in the system.

During this process, a topological ground state with $\sigma_{xy} \times h/e^2 = 1/3$ should undergo two level crossings with the other two gaped topological states (Thouless 1989).

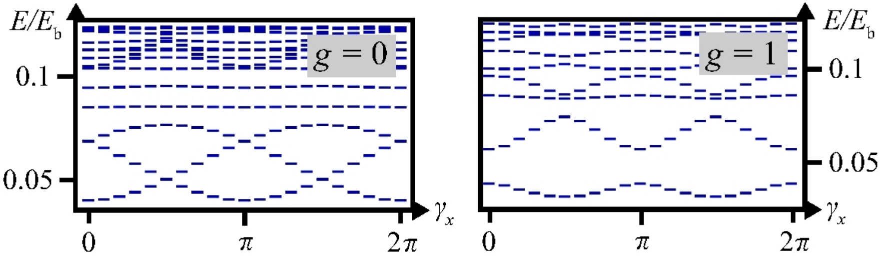

We can now use twisted boundary conditions to probe the topological nature of the ground state: varying γ_x between 0 and 2π is equivalent to the adiabatic insertion of a flux quantum in the system.

During this process, a topological ground state with $\sigma_{xy} \times h/e^2 = 1/3$ should undergo two level crossings with the other two gaped topological states (Thouless 1989).

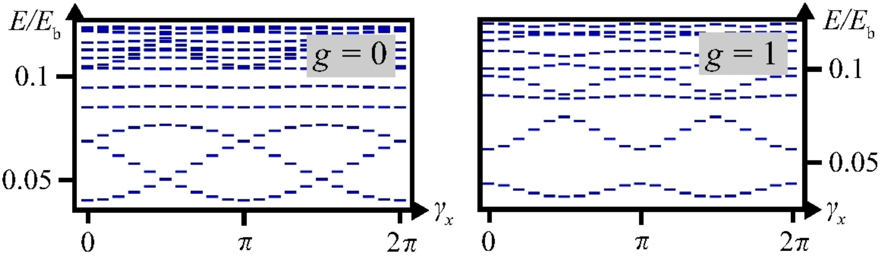

Hall conductance if $N = 3 \times 6$ and $N_{\mathrm{f}} = 6$

The Hall conductance σ_{xy} is related to the Chern-number C of the many-body ground state $|\Psi\rangle$ as

$$\sigma_{xy} = C\, e^2/h$$

where (Niu and Thouless 1984)

$$C := \frac{1}{2\pi \mathrm{i}} \int\limits_{\gamma\in[0,2\pi]^2} \mathrm{d}^2\gamma\, \boldsymbol{\nabla}_\gamma \wedge \left\langle \Psi_\gamma \middle| \boldsymbol{\nabla}_\gamma \middle| \Psi_\gamma \right\rangle .$$

Alternatively, we introduce

$$\widetilde{C} = \frac{1}{2\pi \mathrm{i}} \int\limits_{\boldsymbol{k}\in \mathrm{BZ}} \mathrm{d}^2\boldsymbol{k}\; n_{-,\boldsymbol{k}} \left[\boldsymbol{\nabla}_{\boldsymbol{k}} \wedge \left(\chi^{\dagger}_{-,\boldsymbol{k}} \boldsymbol{\nabla}_{\boldsymbol{k}} \chi_{-,\boldsymbol{k}} \right) \right]$$

where $n_{-,\boldsymbol{k}} = \langle\Psi| c^{\dagger}_{-,\boldsymbol{k}} c_{-,\boldsymbol{k}} |\Psi\rangle$ is the occupation number of the single-particle Bloch state in the lower $(-)$ band with wave vector $\boldsymbol{k}$ evaluated in the many-body ground state.

It can be shown that $C = \widetilde{C}$.

Hall conductance if $N = 3 \times 6$ and $N_{\mathrm{f}} = 6$

The Hall conductance σ_{xy} is related to the Chern-number C of the many-body ground state $|\Psi\rangle$ as

$$\sigma_{xy} = C\, e^2/h$$

where (Niu and Thouless 1984)

$$C := \frac{1}{2\pi \mathrm{i}} \int\limits_{\gamma \in [0,2\pi]^2} \mathrm{d}^2\gamma\ \boldsymbol{\nabla}_{\gamma} \wedge \left\langle \Psi_{\gamma} \left| \boldsymbol{\nabla}_{\gamma} \right| \Psi_{\gamma} \right\rangle .$$

Alternatively, we introduce

$$\widetilde{C} = \frac{1}{2\pi \mathrm{i}} \int\limits_{\boldsymbol{k} \in \mathrm{BZ}} \mathrm{d}^2\boldsymbol{k}\ n_{-,\boldsymbol{k}} \left[\boldsymbol{\nabla}_{\boldsymbol{k}} \wedge \left(\chi^{\dagger}_{-,\boldsymbol{k}} \boldsymbol{\nabla}_{\boldsymbol{k}} \chi_{-,\boldsymbol{k}} \right) \right]$$

where $n_{-,\boldsymbol{k}} = \langle \Psi | c^{\dagger}_{-,\boldsymbol{k}} c_{-,\boldsymbol{k}} | \Psi \rangle$ is the occupation number of the single-particle Bloch state in the lower ($-$) band with wave vector $\boldsymbol{k}$ evaluated in the many-body ground state.

It can be shown that $C = \widetilde{C}$.

Hall conductance if $N = 3 \times 6$ and $N_{\mathrm{f}} = 6$

The Hall conductance σ_{xy} is related to the Chern-number C of the many-body ground state $|\Psi\rangle$ as

$$\sigma_{xy} = C\, e^2/h$$

where (Niu and Thouless 1984)

$$C := \frac{1}{2\pi \mathrm{i}} \int\limits_{\gamma \in [0,2\pi]^2} \mathrm{d}^2\gamma\; \boldsymbol{\nabla}_{\gamma} \wedge \left\langle \Psi_{\gamma} \left| \boldsymbol{\nabla}_{\gamma} \right| \Psi_{\gamma} \right\rangle .$$

Alternatively, we introduce

$$\widetilde{C} = \frac{1}{2\pi \mathrm{i}} \int\limits_{\boldsymbol{k} \in \mathrm{BZ}} \mathrm{d}^2\boldsymbol{k}\; n_{-,\boldsymbol{k}} \left[\boldsymbol{\nabla}_{\boldsymbol{k}} \wedge \left(\chi^{\dagger}_{-,\boldsymbol{k}} \boldsymbol{\nabla}_{\boldsymbol{k}} \chi_{-,\boldsymbol{k}} \right) \right]$$

where $n_{-,\boldsymbol{k}} = \langle \Psi | c^{\dagger}_{-,\boldsymbol{k}} c_{-,\boldsymbol{k}} | \Psi \rangle$ is the occupation number of the single-particle Bloch state in the lower $(-)$ band with wave vector $\boldsymbol{k}$ evaluated in the many-body ground state.

It can be shown that $C = \widetilde{C}$.

When $\mu_s = 0$, $t_2 = t_1/\sqrt{2}$, we find $C = 0.29$ and $\widetilde{C} = 0.30$ and attribute the deviations from $C = 1/3$ to finite-size effects.

When $\mu_s = t_1/\sqrt{2}$, $t_2 = 0$, we find that C and $\widetilde{C}$ vanish to a precision of 10^{-6} and 10^{-3}, respectively.

When $\mu_{\mathrm{s}} = 0$, $t_2 = t_1/\sqrt{2}$, we find $C = 0.29$ and $\widetilde{C} = 0.30$ and attribute the deviations from $C = 1/3$ to finite-size effects.

When $\mu_{\mathrm{s}} = t_1/\sqrt{2}$, $t_2 = 0$, we find that C and $\widetilde{C}$ vanish to a precision of 10^{-6} and 10^{-3}, respectively.

Definition of the lattice model supporting the FQSHE

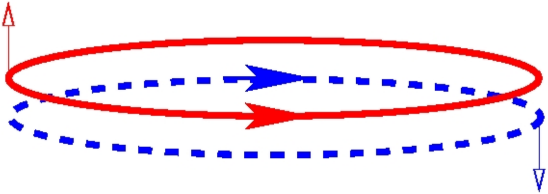

Bernevig and Zhang 2006

Let

$$H_0 := \sum_{\boldsymbol{k}\in\mathrm{BZ}} \left(\psi^\dagger_{\boldsymbol{k},\uparrow} \frac{\boldsymbol{B}_{\boldsymbol{k}}\cdot\boldsymbol{\tau}}{|\boldsymbol{B}_{\boldsymbol{k}}|} \psi_{\boldsymbol{k},\uparrow} + \psi^\dagger_{\boldsymbol{k},\downarrow} \frac{\boldsymbol{B}_{-\boldsymbol{k}}\cdot\boldsymbol{\tau}^{\mathrm{t}}}{|\boldsymbol{B}_{-\boldsymbol{k}}|} \psi_{\boldsymbol{k},\downarrow} \right).$$

This kinetic energy supports the integer QSH quantization $\sigma^{\mathrm{spin}}_{xy} = \pm 2 \times \frac{e}{4\pi}$.

We then choose the interaction

$$H_{\mathrm{int}} := U \sum_{i\in\Lambda} \rho_{i,\uparrow}\rho_{i,\downarrow} + V \sum_{\langle ij\rangle\in\Lambda} \left(\rho_{i,\uparrow}\rho_{j,\uparrow} + \rho_{i,\downarrow}\rho_{j,\downarrow} + 2\lambda \rho_{i,\uparrow}\rho_{j,\downarrow} \right),$$

$U, V \geq 0$.

Definition of the lattice model supporting the FQSHE

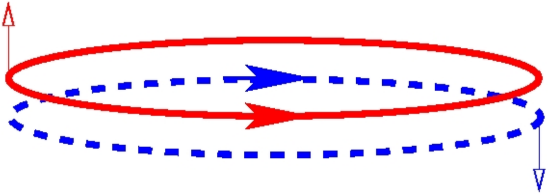

Bernevig and Zhang 2006

Let

$$H_0 := \sum_{\boldsymbol{k}\in\mathrm{BZ}} \left(\psi^{\dagger}_{\boldsymbol{k},\uparrow} \frac{\boldsymbol{B}_{\boldsymbol{k}} \cdot \boldsymbol{\tau}}{|\boldsymbol{B}_{\boldsymbol{k}}|} \psi_{\boldsymbol{k},\uparrow} + \psi^{\dagger}_{\boldsymbol{k},\downarrow} \frac{\boldsymbol{B}_{-\boldsymbol{k}} \cdot \boldsymbol{\tau}^{\mathrm{t}}}{|\boldsymbol{B}_{-\boldsymbol{k}}|} \psi_{\boldsymbol{k},\downarrow} \right).$$

This kinetic energy supports the integer QSH quantization $\sigma^{\mathrm{spin}}_{xy} = \pm 2 \times \frac{e}{4\pi}$.

We then choose the interaction

$$H_{\mathrm{int}} := U \sum_{i\in\Lambda} \rho_{i,\uparrow}\rho_{i,\downarrow} + V \sum_{\langle ij\rangle\in\Lambda} \left(\rho_{i,\uparrow}\rho_{j,\uparrow} + \rho_{i,\downarrow}\rho_{j,\downarrow} + 2\lambda \rho_{i,\uparrow}\rho_{j,\downarrow} \right),$$

$U, V \geq 0$.

Definition of the lattice model supporting the FQSHE

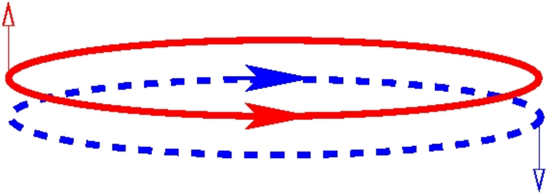

Bernevig and Zhang 2006

Let

$$H_0 := \sum_{\boldsymbol{k}\in\mathrm{BZ}} \left(\psi^\dagger_{\boldsymbol{k},\uparrow} \frac{\boldsymbol{B}_{\boldsymbol{k}}\cdot\boldsymbol{\tau}}{|\boldsymbol{B}_{\boldsymbol{k}}|} \psi_{\boldsymbol{k},\uparrow} + \psi^\dagger_{\boldsymbol{k},\downarrow} \frac{\boldsymbol{B}_{-\boldsymbol{k}}\cdot\boldsymbol{\tau}^{\mathrm{t}}}{|\boldsymbol{B}_{-\boldsymbol{k}}|} \psi_{\boldsymbol{k},\downarrow} \right).$$

This kinetic energy supports the integer QSH quantization $\sigma^{\mathrm{spin}}_{xy} = \pm 2 \times \frac{e}{4\pi}$.

We then choose the interaction

$$H_{\mathrm{int}} := U \sum_{i\in\Lambda} \rho_{i,\uparrow}\rho_{i,\downarrow} + V \sum_{\langle ij\rangle\in\Lambda} \left(\rho_{i,\uparrow}\rho_{j,\uparrow} + \rho_{i,\downarrow}\rho_{j,\downarrow} + 2\lambda\rho_{i,\uparrow}\rho_{j,\downarrow} \right),$$

$U, V \geq 0$.

Definition of the lattice model supporting the FQSHE

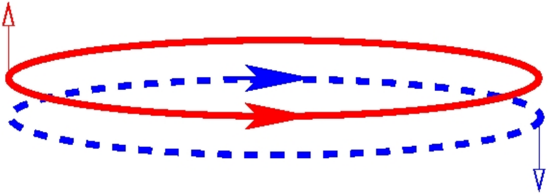

Bernevig and Zhang 2006

Let

$$H_0 := \sum_{\boldsymbol{k}\in\mathrm{BZ}} \left(\psi^{\dagger}_{\boldsymbol{k},\uparrow} \frac{\boldsymbol{B}_{\boldsymbol{k}}\cdot\boldsymbol{\tau}}{|\boldsymbol{B}_{\boldsymbol{k}}|} \psi_{\boldsymbol{k},\uparrow} + \psi^{\dagger}_{\boldsymbol{k},\downarrow} \frac{\boldsymbol{B}_{-\boldsymbol{k}}\cdot\boldsymbol{\tau}^{\mathrm{t}}}{|\boldsymbol{B}_{-\boldsymbol{k}}|} \psi_{\boldsymbol{k},\downarrow} \right).$$

This kinetic energy supports the integer QSH quantization $\sigma^{\mathrm{spin}}_{xy} = \pm 2 \times \frac{e}{4\pi}$.

We then choose the interaction

$$H_{\mathrm{int}} := U \sum_{i\in\Lambda} \rho_{i,\uparrow}\rho_{i,\downarrow} + V \sum_{\langle ij\rangle\in\Lambda} \left(\rho_{i,\uparrow}\rho_{j,\uparrow} + \rho_{i,\downarrow}\rho_{j,\downarrow} + 2\lambda\rho_{i,\uparrow}\rho_{j,\downarrow} \right),$$

$U, V \geq 0$.

Numerical diagonalization

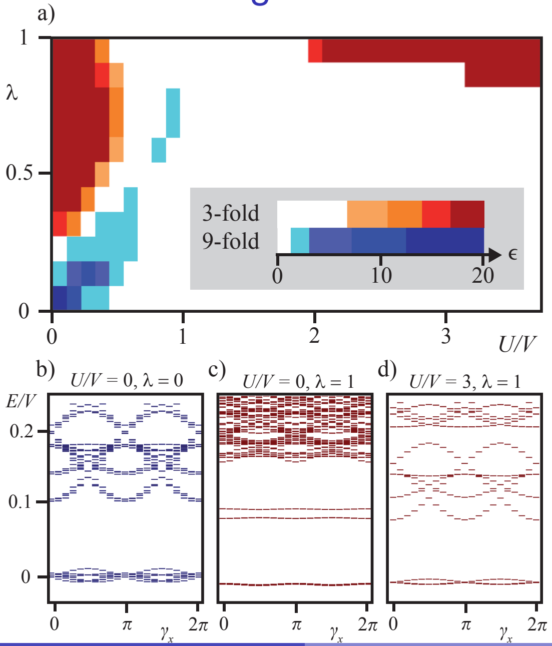

Numerical diagonalization results for 16 electrons when sublattice A is made of 3×4 sites and with $t_2/t_1 = 0.4$. (a) Ground state degeneracies. Denote with E_n the n-th lowest energy eigenvalue of the many-body spectrum where E_1 is the many-body ground state, i.e., $E_{n+1} \geq E_n$ for $n = 1, 2, \cdots$. Define the parameter ϵ by $\epsilon_n := (E_{n+1} - E_n)/(E_n - E_1)$. If a large gap $E_{n+1} - E_n$ opens up between two consecutive levels E_{n+1} and E_n compared to the cumulative level splitting $E_n - E_1$ between the first n many-body eigenstates induced by finite-size effects, then the parameter ϵ_n is much larger than unity. The parameter ϵ_n has been evaluated for $n = 3$ and $n = 9$, yielding the blue and red regions, respectively. For all other $n \neq 1$, no regions with $\epsilon_n \gtrsim O(1)$ of significant size were found. Within the limited range of available system sizes, it is thus not possible to decide on whether and how the level-splitting above the ground state in the white regions of the parameter space extrapolates in the thermodynamic limit. (b)-(d) The lowest eigenvalues with spin-dependent twisted boundary conditions as a function of the twisting angle γ_x. The number of low-lying states that are energetically separated from the other states is 9, 3, and 3, respectively. In panel (c), it is the lowest band parametrized by γ_x that is 3-fold degenerate.

Case $\lambda = U/V = 0$: decoupled FQH states

The model decouples into two FQH-like states at $2/3$ filling, one for each spin orientation.

The low-energy effective theory for this state could be compatible with the choice

$$K = \begin{pmatrix} +1 & +1 & 0 & 0 \\ +1 & -2 & 0 & 0 \\ 0 & 0 & -1 & -1 \\ 0 & 0 & -1 & +2 \end{pmatrix}, \qquad Q = \begin{pmatrix} 1 \\ 0 \\ 1 \\ 0 \end{pmatrix},$$

for the K matrix and the charge vector Q in that it has degeneracy $|\det K| = 3^2 = 9$ as confirmed by the numerical results.

This phase is destabilized by introducing a sufficiently strong coupling between the two FQH states via λ and U.

Case $\lambda = U/V = 0$: decoupled FQH states

The model decouples into two FQH-like states at $2/3$ filling, one for each spin orientation.

The low-energy effective theory for this state could be compatible with the choice

$$K = \begin{pmatrix} +1 & +1 & 0 & 0 \\ +1 & -2 & 0 & 0 \\ 0 & 0 & -1 & -1 \\ 0 & 0 & -1 & +2 \end{pmatrix}, \qquad Q = \begin{pmatrix} 1 \\ 0 \\ 1 \\ 0 \end{pmatrix},$$

for the K matrix and the charge vector Q in that it has degeneracy $|\det K| = 3^2 = 9$ as confirmed by the numerical results.

This phase is destabilized by introducing a sufficiently strong coupling between the two FQH states via λ and U.

Case $\lambda = U/V = 0$: decoupled FQH states

The model decouples into two FQH-like states at $2/3$ filling, one for each spin orientation.

The low-energy effective theory for this state could be compatible with the choice

$$K = \begin{pmatrix} +1 & +1 & 0 & 0 \\ +1 & -2 & 0 & 0 \\ 0 & 0 & -1 & -1 \\ 0 & 0 & -1 & +2 \end{pmatrix}, \qquad Q = \begin{pmatrix} 1 \\ 0 \\ 1 \\ 0 \end{pmatrix},$$

for the K matrix and the charge vector Q in that it has degeneracy $|\det K| = 3^2 = 9$ as confirmed by the numerical results.

This phase is destabilized by introducing a sufficiently strong coupling between the two FQH states via λ and U.

Case $\lambda = 1$, $U/V > 2$: Spontaneous symmetry breaking

We observe that the ground state has the maximal spin-polarization that is allowed by the Pauli principle (Stoner instability).

To interpret this numerical result, first recall that, after projection onto the lowest bands, at most $L_x \times L_y$ electrons may have the same spin, i.e., 12 for the case at hand. Now, the filling fraction is $2/3$, i.e., there are $4/3 \times L_x \times L_y = 16$ electrons. If 12 electrons are fully spin polarized, which is what we observe numerically, then the remaining $1/3 \times L_x \times L_y = 4$ electrons may form a $1/3$ FQH-like state.

We conjecture that the low-energy effective theory for this fully spin-polarized ground state is characterized by the K matrix

$$K = \begin{pmatrix} +1 & 0 \\ 0 & -3 \end{pmatrix}, \qquad Q = \begin{pmatrix} 1 \\ 1 \end{pmatrix}$$

with the filling fraction

$$\nu = Q^{\mathsf{T}} K^{-1} Q = 2/3.$$

This K-matrix does not obey time-reversal symmetry since time-reversal symmetry is spontaneously broken. The degeneracy $|\det K| = 3$ is confirmed by the numerical results. The state thus obtained resembles the conventional double-layer 2/3 FQH state, with the difference that the electron spins are not fully polarized.

Case $\lambda = 1$, $U/V > 2$: Spontaneous symmetry breaking

We observe that the ground state has the maximal spin-polarization that is allowed by the Pauli principle (Stoner instability).

To interpret this numerical result, first recall that, after projection onto the lowest bands, at most $L_x \times L_y$ electrons may have the same spin, i.e., 12 for the case at hand. Now, the filling fraction is $2/3$, i.e., there are $4/3 \times L_x \times L_y = 16$ electrons. If 12 electrons are fully spin polarized, which is what we observe numerically, then the remaining $1/3 \times L_x \times L_y = 4$ electrons may form a $1/3$ FQH-like state.

We conjecture that the low-energy effective theory for this fully spin-polarized ground state is characterized by the K matrix

$$K = \begin{pmatrix} +1 & 0 \\ 0 & -3 \end{pmatrix}, \qquad Q = \begin{pmatrix} 1 \\ 1 \end{pmatrix}$$

with the filling fraction

$$\nu = Q^{\mathsf{T}} K^{-1} Q = 2/3.$$

This K-matrix does not obey time-reversal symmetry since time-reversal symmetry is spontaneously broken. The degeneracy $|\det K| = 3$ is confirmed by the numerical results. The state thus obtained resembles the conventional double-layer 2/3 FQH state, with the difference that the electron spins are not fully polarized.

Case $\lambda = 1$, $U/V > 2$: Spontaneous symmetry breaking

We observe that the ground state has the maximal spin-polarization that is allowed by the Pauli principle (Stoner instability).

To interpret this numerical result, first recall that, after projection onto the lowest bands, at most $L_x \times L_y$ electrons may have the same spin, i.e., 12 for the case at hand. Now, the filling fraction is $2/3$, i.e., there are $4/3 \times L_x \times L_y = 16$ electrons. If 12 electrons are fully spin polarized, which is what we observe numerically, then the remaining $1/3 \times L_x \times L_y = 4$ electrons may form a $1/3$ FQH-like state.

We conjecture that the low-energy effective theory for this fully spin-polarized ground state is characterized by the K matrix

$$K = \begin{pmatrix} +1 & 0 \\ 0 & -3 \end{pmatrix}, \qquad Q = \begin{pmatrix} 1 \\ 1 \end{pmatrix}$$

with the filling fraction

$$\nu = Q^{\mathsf{T}} K^{-1} Q = 2/3.$$

This K-matrix does not obey time-reversal symmetry since time-reversal symmetry is spontaneously broken. The degeneracy $|\det K| = 3$ is confirmed by the numerical results. The state thus obtained resembles the conventional double-layer 2/3 FQH state, with the difference that the electron spins are not fully polarized.

Case $\lambda = 1$, $U/V > 2$: Spontaneous symmetry breaking

We observe that the ground state has the maximal spin-polarization that is allowed by the Pauli principle (Stoner instability).

To interpret this numerical result, first recall that, after projection onto the lowest bands, at most $L_x \times L_y$ electrons may have the same spin, i.e., 12 for the case at hand. Now, the filling fraction is $2/3$, i.e., there are $4/3 \times L_x \times L_y = 16$ electrons. If 12 electrons are fully spin polarized, which is what we observe numerically, then the remaining $1/3 \times L_x \times L_y = 4$ electrons may form a $1/3$ FQH-like state.

We conjecture that the low-energy effective theory for this fully spin-polarized ground state is characterized by the K matrix

$$K = \begin{pmatrix} +1 & 0 \\ 0 & -3 \end{pmatrix}, \qquad Q = \begin{pmatrix} 1 \\ 1 \end{pmatrix}$$

with the filling fraction

$$\nu = Q^{\mathsf{T}} K^{-1} Q = 2/3.$$

This K-matrix does not obey time-reversal symmetry since time-reversal symmetry is spontaneously broken. The degeneracy $|\det K| = 3$ is confirmed by the numerical results. The state thus obtained resembles the conventional double-layer 2/3 FQH state, with the difference that the electron spins are not fully polarized.

Case $\lambda = 1$, $U/V = 0$: Possible paired state

A time-reversal symmetric state with a spectral gap and a 3-fold ground state degeneracy is obtained for small U/V.

This state cannot be captured by the time-reversal symmetric Abelian Chern-Simons theory since its degeneracy is not the square of an integer, despite the time-reversal symmetry.

One may speculate that this state realizes some real-space pairing of spin-up with spin-down electrons, since for small U/V it costs little energy to have two electrons of opposite spin at the same lattice site.

Case $\lambda = 1$, $U/V = 0$: Possible paired state

A time-reversal symmetric state with a spectral gap and a 3-fold ground state degeneracy is obtained for small U/V.

This state cannot be captured by the time-reversal symmetric Abelian Chern-Simons theory since its degeneracy is not the square of an integer, despite the time-reversal symmetry.

One may speculate that this state realizes some real-space pairing of spin-up with spin-down electrons, since for small U/V it costs little energy to have two electrons of opposite spin at the same lattice site.

Case $\lambda = 1$, $U/V = 0$: Possible paired state

A time-reversal symmetric state with a spectral gap and a 3-fold ground state degeneracy is obtained for small U/V.

This state cannot be captured by the time-reversal symmetric Abelian Chern-Simons theory since its degeneracy is not the square of an integer, despite the time-reversal symmetry.

One may speculate that this state realizes some real-space pairing of spin-up with spin-down electrons, since for small U/V it costs little energy to have two electrons of opposite spin at the same lattice site.

Summary

- We have proposed a simple recipe to deform any non-interacting lattice model so as to obtain flat bands, while preserving locality.
- We flattened the bands of the chiral π-flux phase and then lifted the resulting macroscopic ground state degeneracy with repulsive interactions.
- Via exact diagonalization, we have found signatures for a FQH-like topological ground state at 1/3 filling.
- We took the same approach to construct a FQSH-state and found microscopic signatures for it.
- This opens the door for the possibility of realizing dissipativeless charge transport (quantum computing?) at room temperature.

Summary

- We have proposed a simple recipe to deform any non-interacting lattice model so as to obtain flat bands, while preserving locality.
- We flattened the bands of the chiral π-flux phase and then lifted the resulting macroscopic ground state degeneracy with repulsive interactions.
- Via exact diagonalization, we have found signatures for a FQH-like topological ground state at 1/3 filling.
- We took the same approach to construct a FQSH-state and found microscopic signatures for it.
- This opens the door for the possibility of realizing dissipativeless charge transport (quantum computing?) at room temperature.

Summary

- We have proposed a simple recipe to deform any non-interacting lattice model so as to obtain flat bands, while preserving locality.
- We flattened the bands of the chiral π-flux phase and then lifted the resulting macroscopic ground state degeneracy with repulsive interactions.
- Via exact diagonalization, we have found signatures for a FQH-like topological ground state at 1/3 filling.
- We took the same approach to construct a FQSH-state and found microscopic signatures for it.
- This opens the door for the possibility of realizing dissipativeless charge transport (quantum computing?) at room temperature.

Summary

- We have proposed a simple recipe to deform any non-interacting lattice model so as to obtain flat bands, while preserving locality.
- We flattened the bands of the chiral π-flux phase and then lifted the resulting macroscopic ground state degeneracy with repulsive interactions.
- Via exact diagonalization, we have found signatures for a FQH-like topological ground state at 1/3 filling.
- We took the same approach to construct a FQSH-state and found microscopic signatures for it.
- This opens the door for the possibility of realizing dissipativeless charge transport (quantum computing?) at room temperature.

Summary

- We have proposed a simple recipe to deform any non-interacting lattice model so as to obtain flat bands, while preserving locality.
- We flattened the bands of the chiral π-flux phase and then lifted the resulting macroscopic ground state degeneracy with repulsive interactions.
- Via exact diagonalization, we have found signatures for a FQH-like topological ground state at 1/3 filling.
- We took the same approach to construct a FQSH-state and found microscopic signatures for it.
- This opens the door for the possibility of realizing dissipativeless charge transport (quantum computing?) at room temperature.

Summary

- We have proposed a simple recipe to deform any non-interacting lattice model so as to obtain flat bands, while preserving locality.
- We flattened the bands of the chiral π-flux phase and then lifted the resulting macroscopic ground state degeneracy with repulsive interactions.
- Via exact diagonalization, we have found signatures for a FQH-like topological ground state at 1/3 filling.
- We took the same approach to construct a FQSH-state and found microscopic signatures for it.
- This opens the door for the possibility of realizing dissipativeless charge transport (quantum computing?) at room temperature.

Bulk time-reversal symmetric effective theory (Abelian)

Define $S := S_0 + S_e + S_s$ with

$$S_0 := -\int \mathrm{d}t\,\mathrm{d}^2\boldsymbol{x}\;\epsilon^{\mu\nu\rho}\,\frac{1}{4\pi}K_{ij}\;a^i_\mu\;\partial_\nu\;a^j_\rho,$$

$$S_e := +\int \mathrm{d}t\,\mathrm{d}^2\boldsymbol{x}\;\epsilon^{\mu\nu\rho}\,\frac{e}{2\pi}\;Q_i\;A_\mu\partial_\nu\;a^i_\rho,$$

$$S_s := +\int \mathrm{d}t\,\mathrm{d}^2\boldsymbol{x}\;\epsilon^{\mu\nu\rho}\,\frac{s}{2\pi}\;S_i\;B_\mu\partial_\nu\;a^i_\rho,$$

and

$$K = \begin{pmatrix} \kappa & \Delta \\ \Delta^{\mathsf{T}} & -\kappa \end{pmatrix}, \qquad \kappa^{\mathsf{T}} = \kappa \in \mathrm{GL}(N,\mathbb{Z}), \qquad \Delta^{\mathsf{T}} = -\Delta \in \mathrm{GL}(N,\mathbb{Z}),$$

$$Q = \begin{pmatrix} \varrho \\ \varrho \end{pmatrix} \in \mathbb{Z}^{2N}, \qquad S = \begin{pmatrix} \varrho \\ -\varrho \end{pmatrix} \in \mathbb{Z}^{2N}, \qquad (-)^{Q_i} = (-)^{K_{ii}}.$$

Then

$$\nu_e := Q^{\mathsf{T}}\;K^{-1}\;Q = 0, \qquad \nu_s := \frac{1}{2}\,Q^{\mathsf{T}}\;K^{-1}\;S \neq 0, \qquad \sigma_{\mathrm{sH}} := \frac{e}{2\pi}\times\nu_s.$$

Wave function for $N = 1$

If

$$K = \begin{pmatrix} +m & 0 \\ 0 & -m \end{pmatrix} \in \mathrm{GL}(2, \mathbb{Z}), \qquad Q = \begin{pmatrix} 1 \\ 1 \end{pmatrix} \in \mathbb{Z}^2,$$

for some given positive odd integer m, then

$$\nu_{\mathrm{s}} = \frac{1}{m}$$

and

$$\Psi_{1/m}(\{z, \bar{z}\}_n \,|\, \{w, \bar{w}\}_n) = \left[\prod_{i=1}^{n} \prod_{j=i+1}^{n} \left(z_i - z_j\right)^m \left(\bar{w}_i - \bar{w}_j\right)^m\right] \prod_{i=1}^{n} \exp\left(-\frac{|z_i|^2 + |\bar{w}_i|^2}{4\ell^2}\right).$$

Wave function in the symmetric representation for $N = 2$

If

$$K = \begin{pmatrix} +\begin{pmatrix} m_1 & n \\ n & m_2 \end{pmatrix} & +\begin{pmatrix} 0 & +d \\ -d & 0 \end{pmatrix} \\ -\begin{pmatrix} 0 & +d \\ -d & 0 \end{pmatrix} & -\begin{pmatrix} m_1 & n \\ n & m_2 \end{pmatrix} \end{pmatrix} \in \mathrm{GL}(4,\mathbb{Z}), \qquad Q = \begin{pmatrix} 1 \\ 1 \\ 1 \\ 1 \end{pmatrix} \in \mathbb{Z}^4,$$

with $m_1 m_2 - n^2 > 0$, then

$$\nu_{\mathrm{s}} = \frac{m_1 + m_2 - 2n}{m_1\, m_2 - n^2 + d^2}$$

and [generalization of Halperin's (m_1, m_2, n) bilayer function]

$$\begin{aligned} \Psi^{\mathrm{symm}}_{m_1,m_2,n,d}\left(\{z_1,\bar{z}_1\}_{n_1};\{z_2,\bar{z}_2\}_{n_2}\,|\,\{w_1,\bar{w}_1\}_{n_1};\{w_2,\bar{w}_2\}_{n_2}\right) = \\ \Psi_{1/m_1}\left(\{z_1,\bar{z}_1\}_{n_1}\,|\,\{w_1,\bar{w}_1\}_{n_1}\right) \times \Psi_{1/m_2}\left(\{z_2,\bar{z}_2\}_{n_2}\,|\,\{w_2,\bar{w}_2\}_{n_2}\right) \\ \times \prod_{i=1}^{n_1}\prod_{j=1}^{n_2}\left(z_{1,i}-z_{2,j}\right)^n\left(\bar{w}_{1,i}-\bar{w}_{2,j}\right)^n\left(z_{1,i}-w_{2,j}\right)^d\left(\bar{w}_{1,i}-\bar{z}_{2,j}\right)^d. \end{aligned}$$

Wave function in the hierarchical representation for $N = 2$

If

$$K = \begin{pmatrix} +\begin{pmatrix} +m & +1 \\ +1 & -p \end{pmatrix} & +\begin{pmatrix} 0 & +d \\ -d & 0 \end{pmatrix} \\ -\begin{pmatrix} 0 & +d \\ -d & 0 \end{pmatrix} & -\begin{pmatrix} +m & +1 \\ +1 & -p \end{pmatrix} \end{pmatrix} \in \mathrm{GL}(4, \mathbb{Z}), \qquad Q = \begin{pmatrix} 1 \\ 0 \\ 1 \\ 0 \end{pmatrix} \in \mathbb{Z}^4,$$

with m a positive odd integer and p an even integer then

$$\nu_{\mathrm{s}} = \frac{p}{mp + 1 - d^2}$$

and [generalization of Halperin's $\nu = p/(mp+1)$ bilayer function]

$$\Psi^{\mathrm{hier}}_{m,-p,1,d}\left(\{z,\bar{z}\}_{pn} \,|\, \{w,\bar{w}\}_{pn}\right) =$$

$$\left[\prod_{i=1}^{n} \int_{\Omega} \mathrm{d}^2\,\eta_i \int_{\Omega} \mathrm{d}^2\,\xi_i\right] \times \Psi_{1/m}\left(\{z,\bar{z}\}_{pn} \,|\, \{w,\bar{w}\}_{pn}\right) \times \Psi_{1/p}\left(\{\xi,\bar{\xi}\}_{n} \,|\, \{\eta,\bar{\eta}\}_{n}\right)$$

$$\times \prod_{i=1}^{pn} \prod_{j=1}^{n} \left(z_i - \eta_j\right)\left(\bar{w}_i - \bar{\xi}_j\right)\left(z_i - \xi_j\right)^d \left(\bar{w}_i - \bar{\eta}_j\right)^d .$$

Edge theory with time-reversal symmetry

The bulk action with a two-body and translation-invariant interaction is equivalent to

$$\hat{H}_0 := \int_0^L \mathrm{d}x \, \frac{1}{4\pi} \partial_x \hat{\Phi}^{\mathsf{T}} \; V \, \partial_x \hat{\Phi}$$

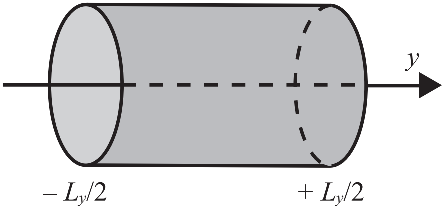

where V is a $2N \times 2N$ symmetric and positive definite matrix and

$$\left[\hat{\Phi}_i(t,x), \hat{\Phi}_j(t,x')\right] = -\mathrm{i}\pi\left(K^{-1}_{ij} \,\mathrm{sgn}(x-x') + \Theta_{ij}\right).$$

Here,

$$\Theta_{ij} := K^{-1}_{ik} \, L_{kl} \, K^{-1}_{lj}$$

and the antisymmetric $2N \times 2N$ matrix L is defined by (Haldane 1995)

$$L_{ij} = \mathrm{sgn}(i-j) \left(K_{ij} + Q_i \, Q_j\right),$$

where $\mathrm{sgn}(0) = 0$ is understood.

Tunneling of electronic charge among the different edge branches is

$$\hat{H}_{\rm int} := -\int\limits_0^L \mathrm{d}x \sum_{T\in\mathbb{L}} h_T(x) : \cos\left(T^{\mathsf{T}} K\, \hat{\Phi}(x) + \alpha_T(x)\right) : \ .$$

The real functions $h_T(x) \geq 0$ and $0 \leq \alpha_T(x) \leq 2\pi$ encode information about the disorder along the edge when position dependent. The set

$$\mathbb{L} := \left\{ T \in \mathbb{Z}^{2N} \,\middle|\, T^{\mathsf{T}} Q = 0 \right\}$$

encodes all the possible charge neutral tunneling processes, i.e., those that just rearrange charge among the branches.
At least one pair of Kramers degenerate edge state remains delocalized along the edge described by $\hat{H} := \hat{H}_0 + \hat{H}_{\rm int}$ if the integer

$$R := r\, \varrho^{\mathsf{T}}\, (\kappa - \Delta)^{-1}\, \varrho$$

is odd. Here, the integer r is the smallest integer such that all the N components of the vector $r\, (\kappa - \Delta)^{-1}\, \varrho$ are integers.